Solving flow problems since 1894

Northfield Mountain Generation Station (FERC No. 2485), CFD Modeling for Fish Exclusion Net Forces

Alden Report No. : 3184NMPSPBN

Prepared for:

June 2019

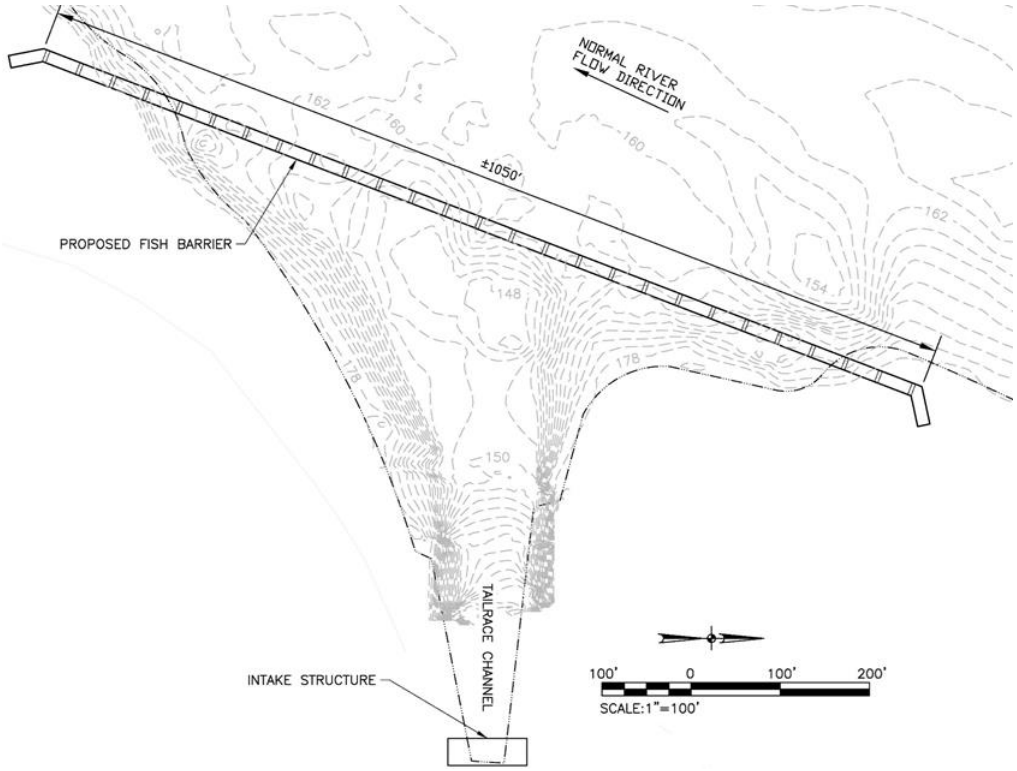

ALDEN Research Laboratory, Inc.

30 Shrewsbury Street, Holden, Massachusetts
01520-1843

Massachusetts | Colorado | Oregon | Washington

508-829-6000 • www.aldenlab.com

Signature Block

Name/Title	Signature/Date	Preparer (P) Reviewer (R)
Farid Karimpour, Ph.D. Engineer II	05/10/19	P
Daniel Gessler, P.E., Ph.D., D.WRE Vice President	05/10/19	R

Record of Revisions

Revision No.	Revision Date	Change Description	Reason for Change
1	1/11/2019	Initial Issue	
2	05/09/2019	Revised Report	Address comments

Table of Contents

List of Figures

List of Tables

Executive Summary

The Northfield Mountain Pumped-Storage Project (Project, FERC No. 2485) is located on the Connecticut River in both Erving and Northfield, Massachusetts. It is owned and operated by FirstLight Hydro Generating Company (FirstLight). The Project consists of a lower reservoir, called the Turners Falls Impoundment (TFI) that is created by the Turners Falls Dam, and an Upper Reservoir atop Northfield Mountain. Pending energy demands, water is typically pumped from the TFI to the Upper Reservoir at night, when energy demand is lower, and is used for generation during the day, when the demand is higher. When operating in a pumping mode the four equally-sized pump-turbines have a total hydraulic capacity of approximately 15,200 cfs. In the generating mode the four turbines have a total hydraulic discharge capacity of approximately 20,000 cfs.

The hydropower facilities at Turners Falls are equipped with upstream and downstream migratory fish passage facilities that can pass resident and diadromous fish, including American shad and American eel. There is the potential for further modifications and/or improvements to these fish passage structures as part of the Federal Energy Regulatory Commission (FERC) relicensing process. The resources agencies have raised concerns that when the Northfield Mountain Project operates in a pumping mode, migratory fish can be entrained and lost from the river system.

As part of the FERC relicensing process, FirstLight is considering installing a fish exclusion net in the TFI at the Northfield Project intake/tailwater to protect outmigrating juvenile American shad and adult American eel from becoming entrained during pumping. FirstLight's concern is the likelihood of plugging the exclusion net in the summer (when bio-fouling of the net is a concern) and fall (when leaf-off occurs), and the potential impacts on its ability to pump or generate with all four units. As part of its consideration of this potential Protection, Mitigation and Enhancement (PME) measure, FirstLight requested Alden Research Laboratory, Inc. (Alden) to conduct a study to determine forces acting on a fish exclusion net deployed at the Northfield Project intake/ tailwater, considering biofouling, to support FirstLight's determination of feasibility.

Design of the exclusion net requires determination of the forces acting on the net when in full pumping or generating mode. To determine forces, numerical simulations were performed, which required prescription of drag coefficients in the model. To determine drag coefficients, sample nets were deployed in the Connecticut River (TFI) upstream of the Northfield tailrace to assess algae growth and bio-fouling effects. The sample nets were brought to the laboratory to determine the drag coefficients, which were used in the numerical model. Alden previously developed a three-dimensional Computational Fluid Dynamics (CFD) model of the intake/tailwater to numerically study sediment exclusion strategies (Ref. 9.0). The CFD model was used to simulate the flow patterns and to determine the forces acting on the net. Combinations of plant operating conditions and river flow conditions expected to yield high hydraulic forces acting on the exclusion net were selected for simulation. Flow conditions were tested with both Project pumping and generating operations. The hydraulic forces acting on

the exclusion net were computed at the location of the exclusion net. This report summarizes the CFD modeling effort and hydraulic forces calculations of the exclusion net.

An initial set of CFD modeling runs were conducted to evaluate forces on the net and velocities in front of the net including:

- Maximum pumping flow of 15,200 cfs and maximum generating flow of 20,000 cfs;
- Different magnitudes of flow in the Connecticut River passing by the Northfield intake/tailrace including 5,000 cfs, 30,000 and 50,000 cfs; and,
- Different intake/tailrace elevations including 179, 182 and 185 feet (NGVD29 datum)

The above scenarios were simulated with a composite net, consisting of 3/8-inch mesh on the top and 0.75-inch on the bottom over the length of the net. In addition to the forces on the net, the normal and tangential velocities in front of the net were computed and compared to the United States Fish and Wildlife Service guideline of 2 feet/second. Some portions of the net exceeded the 2.0 foot/second guideline. After the initial set of runs were complete, additional simulations were conducted with a 0.75-inch mesh net from top to bottom. By having a larger mesh size, the forces on the net were reduced. Note that FirstLight proposes that any exclusion net will be 0.75-inch mesh from top to bottom.

The next steps are to review the velocity results with the agencies, solicit their feedback, and determine if modifications to the conceptual layout is needed.

1.0 Introduction

The Northfield Mountain Pumped-Storage Project (Project, FERC No. 2485) is located on the Connecticut River, in both Erving and Northfield, Massachusetts. The Project location is shown in Figure 1-1. Figure 1-2 shows a more detailed aerial view of the Northfield intake/tailwater area.

FirstLight is reviewing the efficacy of an exclusion net deployed in front of the intake/tailwater to exclude outmigrating fish from being entrained during pumping operations. The exclusion net would be deployed between August 1 and November 15 to protect migratory juvenile American shad and adult American eel. Based on preliminary calculations to maintain average intake velocities less than 2 ft/sec, the proposed exclusion net would span about 1,000 ft of the intake/tailwater entrance as shown in Figure 1-3. Figure 1-4 shows an elevation view of the proposed net detailing the upper net panel (3/8-inch mesh size) and lower net panel (0.75-inch mesh size). Note that although Figures 1-4 shows a composite net, FirstLight proposes that any exclusion net will be 0.75-inch mesh from top to bottom. As described later, an assessment of the exclusion net with 0.75-inch mesh size from top to bottom was also evaluated. The purpose of this Computational Fluid Dynamics (CFD) modeling study was to evaluate hydraulic forces acting on the exclusion net under a range of river flow conditions, water elevations at the Project intake/tailrace, various Project maximum pumping and generating capacities and with different mesh sizes. The study also provided information on the normal and tangential velocities at the exclusion net to determine if velocities were less 2 ft/sec.

The current CFD model study leveraged past modeling efforts to determine the velocity field near the proposed exclusion net. Alden previously developed a three-dimensional CFD hydraulic model of the intake/tailwater to study sediment exclusion strategies (Ref. 9.0). The CFD model extends approximately 1,200 ft upstream and 1,000 ft downstream from the Project intake/tailwater. Nets are modeled as flat porous baffles in the CFD simulations and the hydraulic forces acting on them were then calculated.

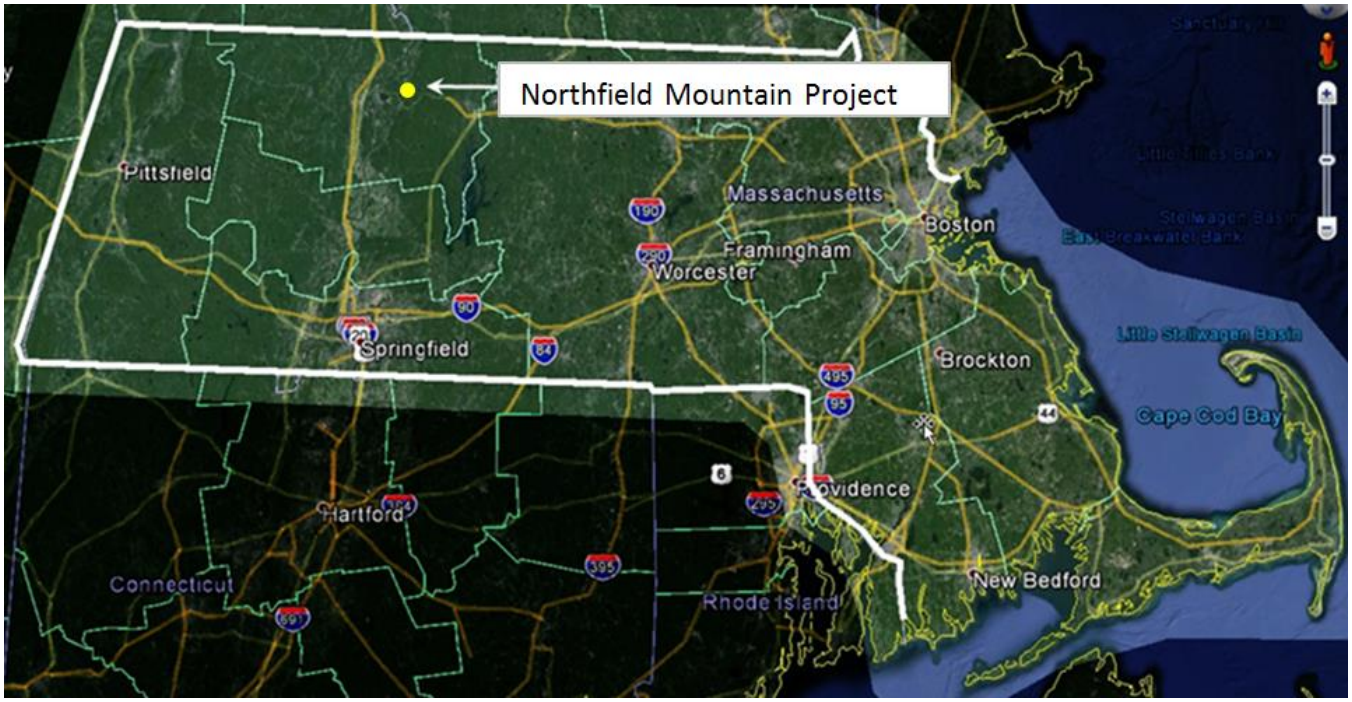

Figure 1-1. Northfield Mountain project location map

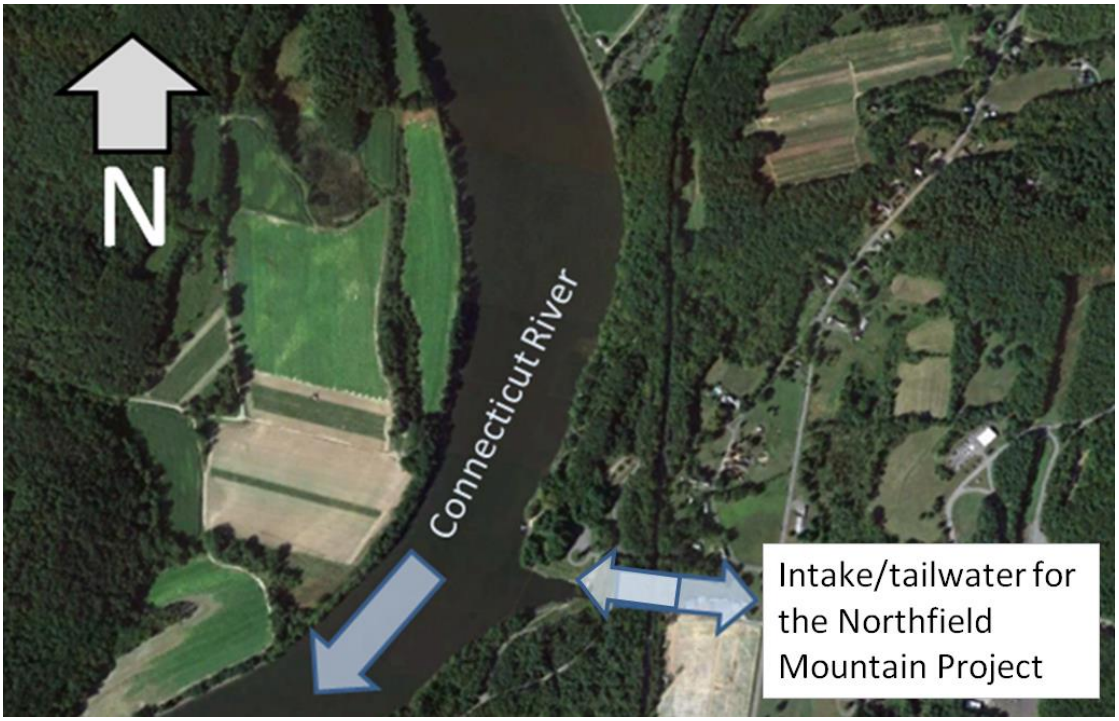

Figure 1-2. Detail of Northfield Mountain project intake/tailwater

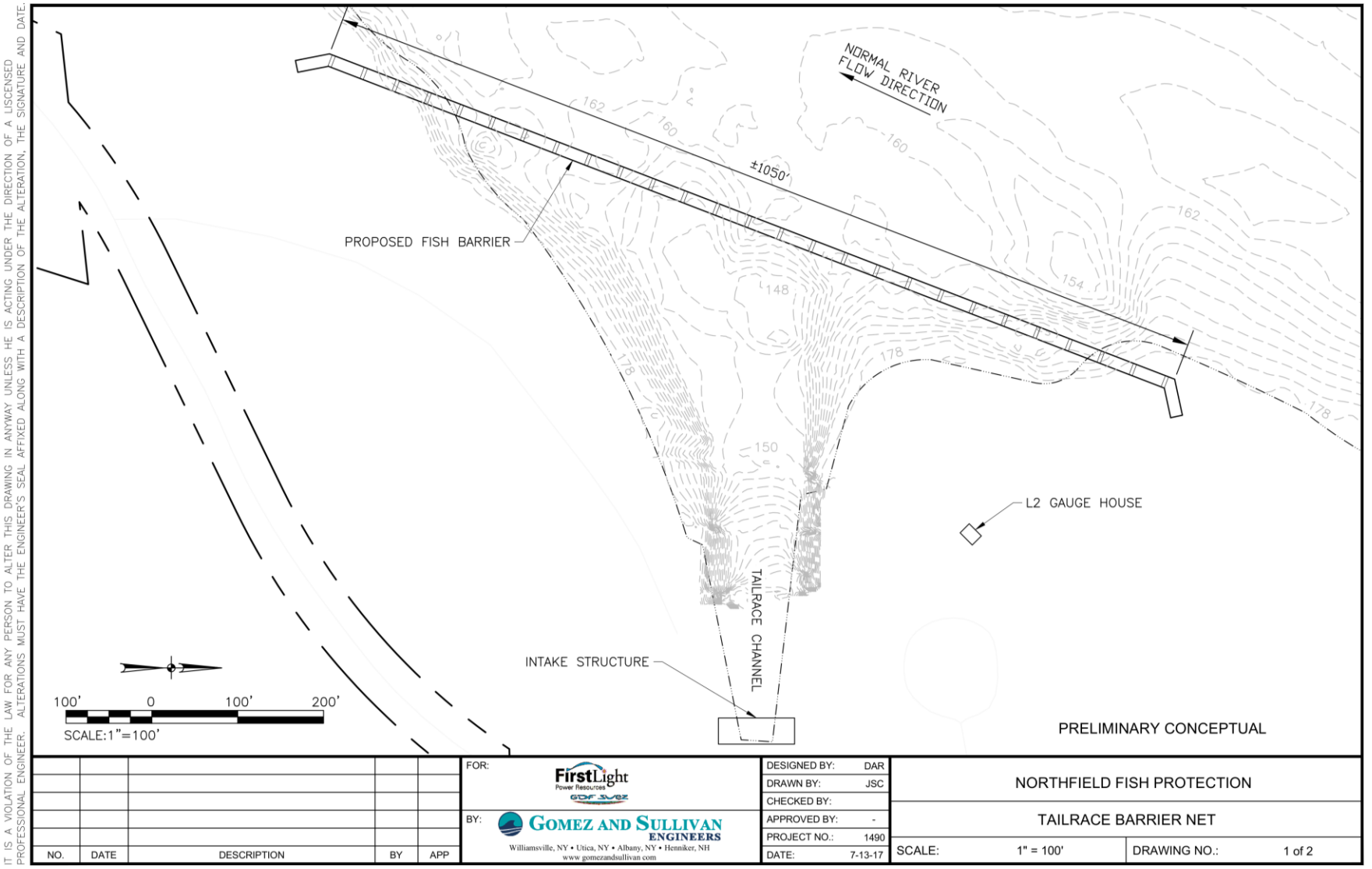

Figure 1-3. Exclusion net plan view (Ref. [2])

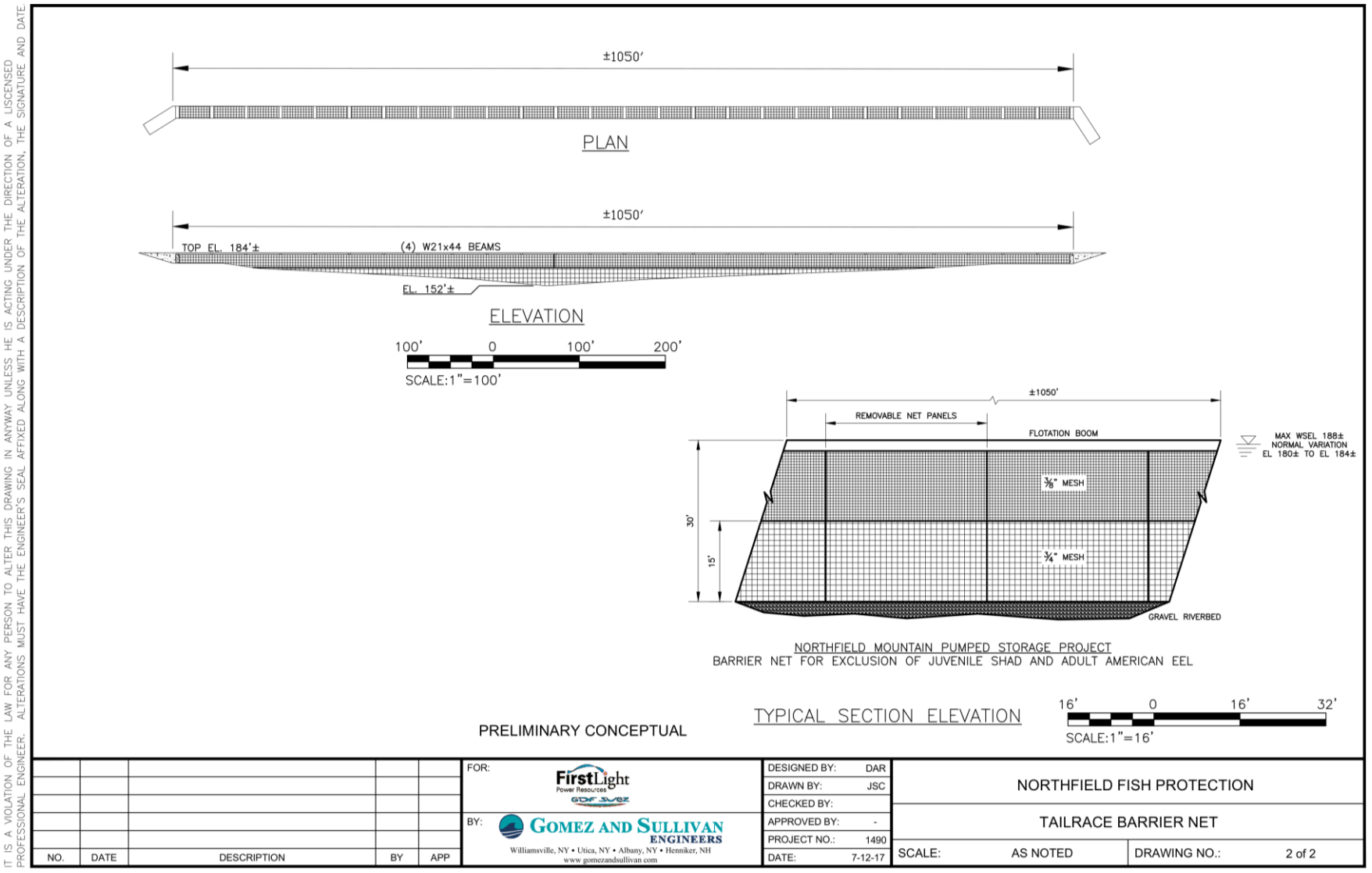

Figure 1-4. Exclusion net elevation (Ref. [2]). The top net size is 3/8'' and the bottom net size is 0.75''.

2.0 Model Selection

It is necessary to calculate the hydraulic forces acting on the exclusion net to design the anchoring system. In principal, the drag on the net could be determined using a reduced scale physical model such as the one Alden constructed for testing sediment exclusion concepts in the Project intake/tailrace. A physical model of the netting would deform in response to the hydraulic forces and the flow field would adjust to the forces exerted by the netting. In theory, the tensile forces on cables and anchoring systems could be measured in a scale model. However, the existing 1:100 model is too small and cannot be used for this purpose because the sizing limitations do not allow to properly satisfy scaling requirements, such as Reynolds similitude, which is discussed in more detail below. In the field, flow through the exclusion net is expected to be in the fully turbulent flow regime as defined by the net Reynolds number. The pore Reynolds number Re for flow through the net openings is

$$Re = \frac{u_{pore} D}{\nu}, \qquad (1)$$

where u_{pore} is the pore velocity through the net, D is the mesh opening size, and ν = 1.21×(10)$^{-5}$ ft^2/s is the kinematic viscosity of water. The pore velocity u_{pore} is defined as

$$u_{pore} = u_{norm}/\phi_{open}, \qquad (2)$$

where u_{norm} is the normal velocity (i.e. approach velocity) and ϕ_{open} is the porosity, which is the ratio of open to the total area (i.e. $\phi = A_o/A_T$, where A_o is the open area and A_T is the total area of the net). For the 0.75-inch mesh size, $D \approx$ 0.65 inch and ϕ_{open} = 0.751 (Ref. [3]). If u_{norm} = 1 ft/s then the pore Reynolds number is 6,000 which is fully turbulent. If we use Froude similitude (i.e. prototype Froude number is equal to model Froude number), and the ratio of physical model length scale to prototype length scale is assumed to be 1:100, then the physical model velocity to prototype velocity ratio is 1:10. For this condition, the pore Reynolds number is 6.0 for the model scale. The flow is laminar when the pore Reynolds number is less than 200 and turbulent when the pore Reynolds number is greater than 1,000. It is critical that the turbulence regime and Reynolds number of the actual net matches the physical model for the hydraulic forces acting on the exclusion net to scale reliably. If the actual mesh size is used in the physical model, then with the physical model to prototype velocity ratio 1:10, the model pore Reynolds number is 600 which is in the laminar-turbulent transition regime and does not match the fully turbulent regime. Additionally, the total force on the net in the physical model is (Pressure) × (Area) and scales as (velocity squared) × (length squared) = (1:10)^2 × (1:100)^2 = 1:1,000,000. Measuring forces 1,000,000 times smaller than the full-size net is not feasible. Thus, due to different turbulence regimes and difficulty of measuring considerably small forces, it is not feasible to use the existing physical model to determine the hydraulic forces on the exclusion net. Therefore, it was necessary to approximate the forces on the exclusion net from the velocity field determined from a CFD model.

3.0 Laboratory Tests: Determining Drag Coefficients

In the CFD simulations, the net was modeled as a porous baffle, which required defining the porosity and the drag coefficient. To do so, sample nets similar to the exclusion nets with 1) mesh size = 3/8'' and porosity $\phi = 0.586$; and 2) mesh size = 0.75'' and porosity $= 0.751$ were considered. The drag coefficients were determined by performing lab tests on 3/8-inch and 0.75-inch sample net panels. In order to assess the effect of bio-fouling on the exclusion net, sample net panels were deployed at the exclusion net location in the TFI just north (upstream) of the Project intake/tailwater. The sample net panels were deployed at the top, middle, and bottom of the water column with various residence times:

1) panels with clean screen, i.e. not deployed (sample net panels deployment was July 25th 2018);

2) sample net panels floating in water for 27 days, removed on August 21st;

3) sample net panels floating in water for 50 days, removed on September 13th;

4) sample net panels floating in water for 82 days, removed on October 15th; and

5) sample net panels floating in water for 113 days, removed on November 14th.

The sample nets were then tested in a flume in the lab to determine the drag coefficients. The tests were performed for different approach velocities (~0.5, 1.0, 1.5, 2.0 ft/s) and the corresponding acting forces, head loss as well as wetted area, were measured. Figure 3-1 (a) shows the sample net panel and the bio-fouling effect and Figure 3-1 (b) represents the tests performed in the laboratory flume.

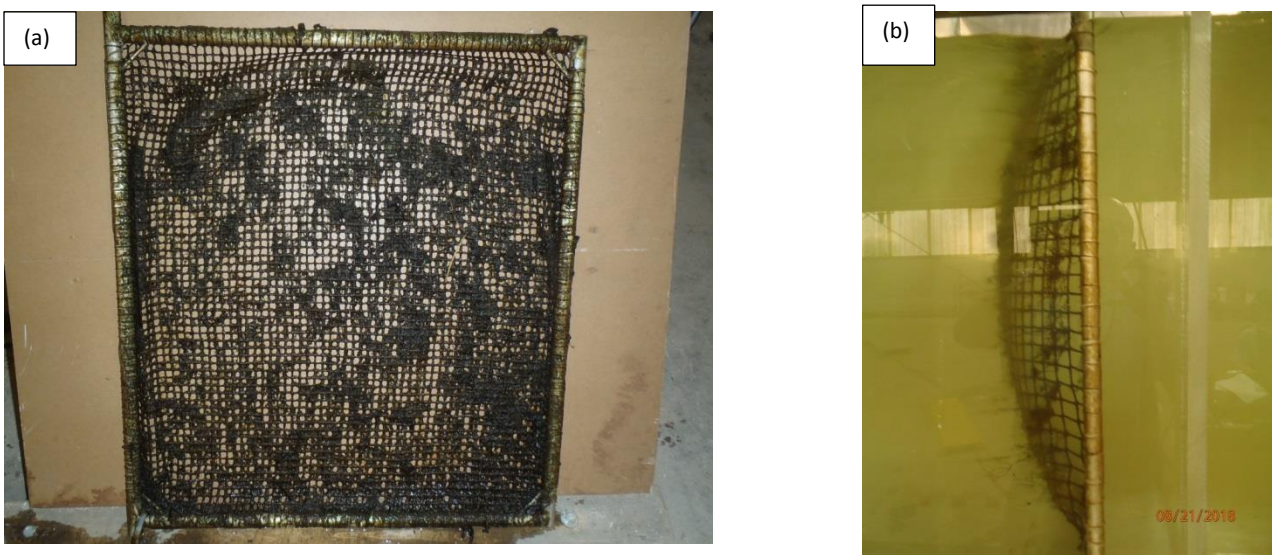

Figure 3-1. (a) The effect of bio-fouling on the sample net, (b) The test of the sample net panel in the lab flume.

3.1 Drag coefficients

Drag force is the force that an object in a moving fluid experiences due to pressure and shear stress forces acting on the surface of the object. Drag force is calculated as:

$$F = 1/2\rho C_d u_0|u_0|A, \quad (1)$$

where F is the force exerted on the object, $\rho = 1.94$ slug is the water density, C_d is the drag coefficient, u_0 is the approach velocity and A is the object's projected area on a plane normal to the flow. Measuring the force and approach velocity in the lab experiments, the drag coefficients are calculated as:

$$C_d = 2F/(\rho u_0^2 A). \quad (2)$$

Calculated drag coefficients based on laboratory data for different residence times of the net panels are provided in Figures 3-2, 3-3, 3-4 and 3-5.

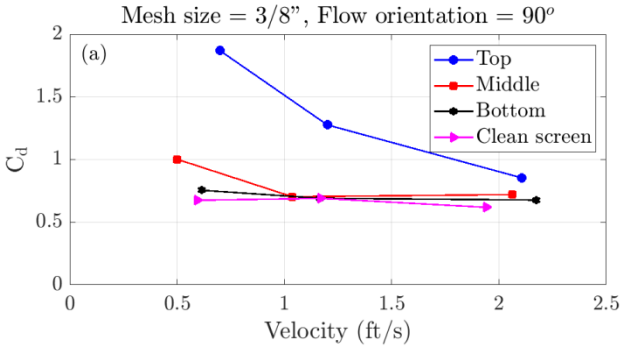
Mesh size = 3/8", Flow orientation = 90°
(a)
Top
Middle
Bottom
Clean screen
C_d
Velocity (ft/s)

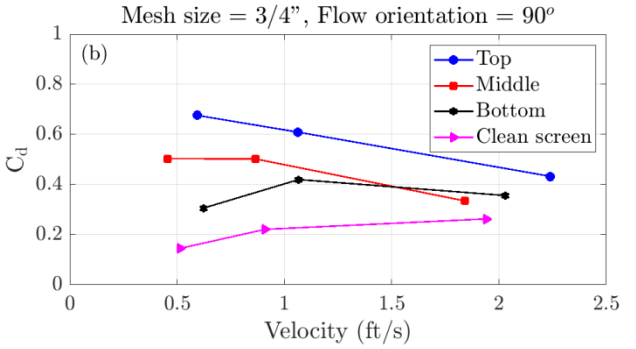
Mesh size = 3/4", Flow orientation = 90°
(b)
Top
Middle
Bottom
Clean screen
C_d
Velocity (ft/s)

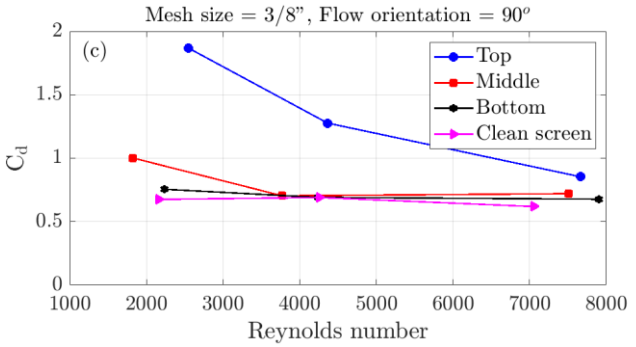
Mesh size = 3/8", Flow orientation = 90°
(c)
Top
Middle
Bottom
Clean screen
C_d
Reynolds number

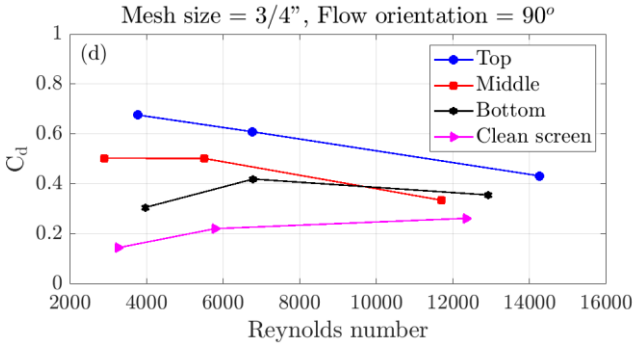
Mesh size = 3/4", Flow orientation = 90°
(d)
Top
Middle
Bottom
Clean screen
C_d
Reynolds number

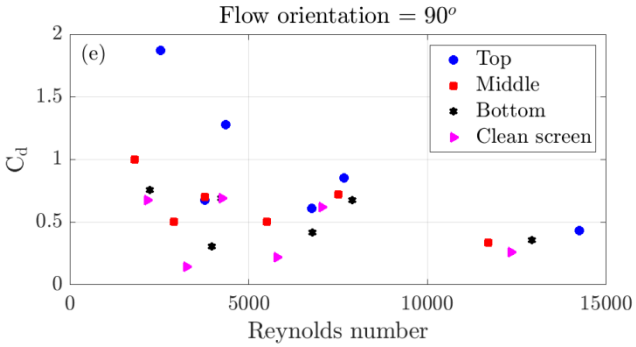

Figure 3-2. The sample nets drag coefficient for clean screen and also 27 days after deployment in water (a) Drag coefficient versus velocity for mesh size 0.375-inch, (b) Drag coefficient versus velocity for mesh size 0.750-inch, (c) Drag coefficient versus Reynolds number for mesh size 0.375-inch, (d) Drag coefficient versus Reynolds number for mesh size 0.750-inch, (e) Drag coefficient versus Reynolds number for mesh size 0.375-inch and 0.750-inch.

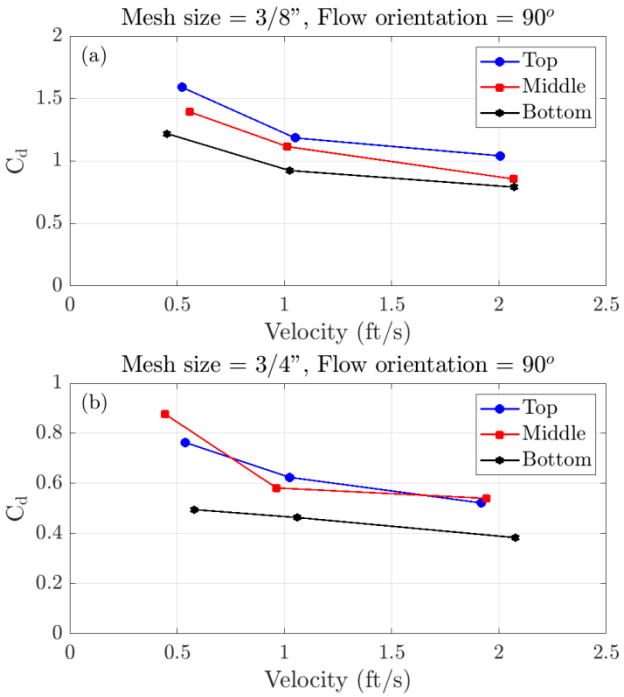

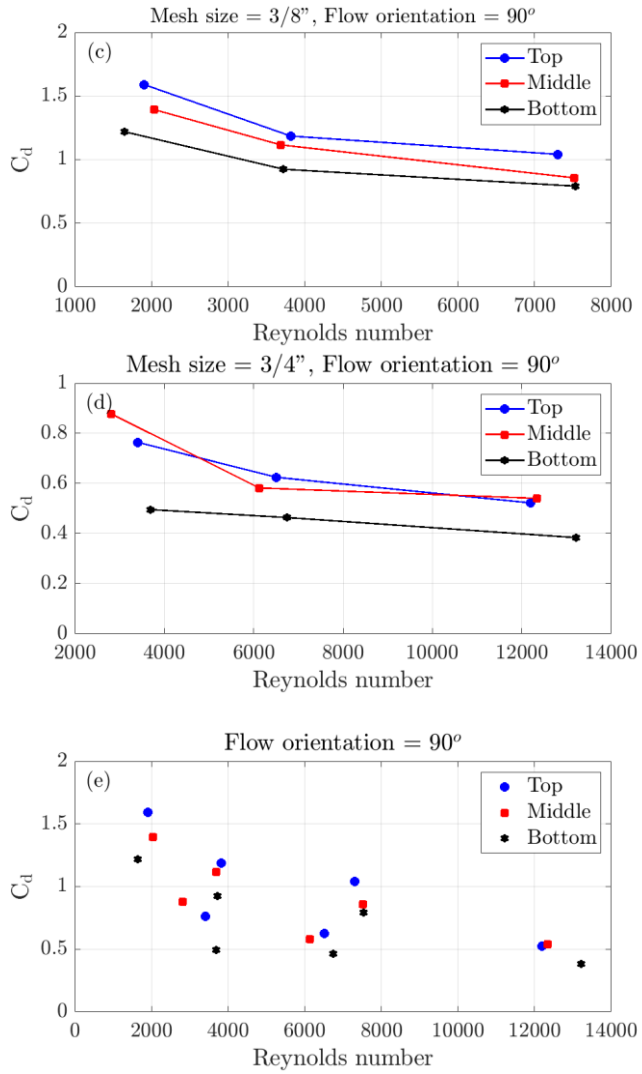

Figure 3-3. The sample nets drag coefficient for 50 days after deployment in water (a) Drag coefficient versus velocity for mesh size 0.375-inch, (b) Drag coefficient versus velocity for mesh size 0.750-inch, (c) Drag coefficient versus Reynolds number for mesh size 0.375-inch, (d) Drag coefficient versus Reynolds number for mesh size 0.750-inch, (e) Drag coefficient versus Reynolds number for mesh size 0.375-inch and 0.750-inch.

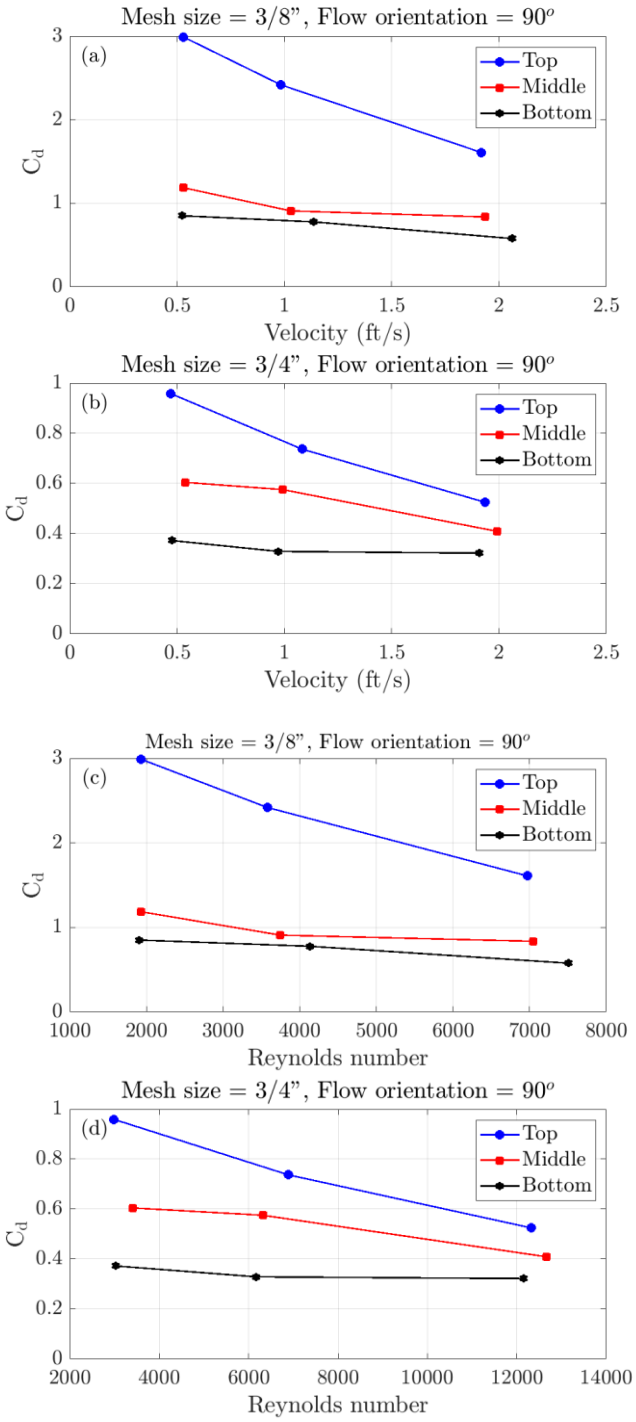
Mesh size = 3/8", Flow orientation = 90°
(a)
Top
Middle
Bottom
C_d
Velocity (ft/s)
Mesh size = 3/4", Flow orientation = 90°
(b)
Top
Middle
Bottom
C_d
Velocity (ft/s)
Mesh size = 3/8", Flow orientation = 90°
(c)
Top
Middle
Bottom
C_d
Reynolds number
Mesh size = 3/4", Flow orientation = 90°
(d)
Top
Middle
Bottom
C_d
Reynolds number

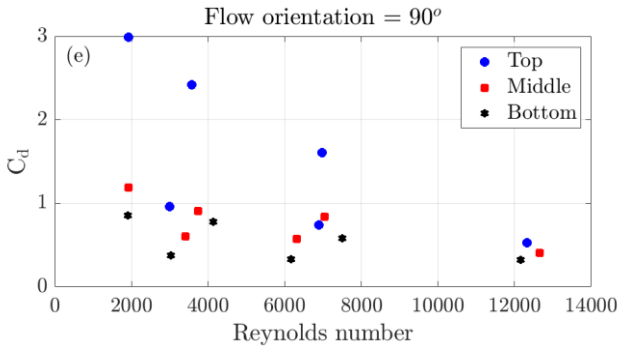

Figure 3-4. The sample nets drag coefficient for 82 days after deployment in water (a) Drag coefficient versus velocity for mesh size 0.375-inch, (b) Drag coefficient versus velocity for mesh size 0.750-inch, (c) Drag coefficient versus Reynolds number for mesh size 0.375-inch, (d) Drag coefficient versus Reynolds number for mesh size 0.750-inch, (e) Drag coefficient versus Reynolds number for mesh size 0.375-inch and 0.750-inch.

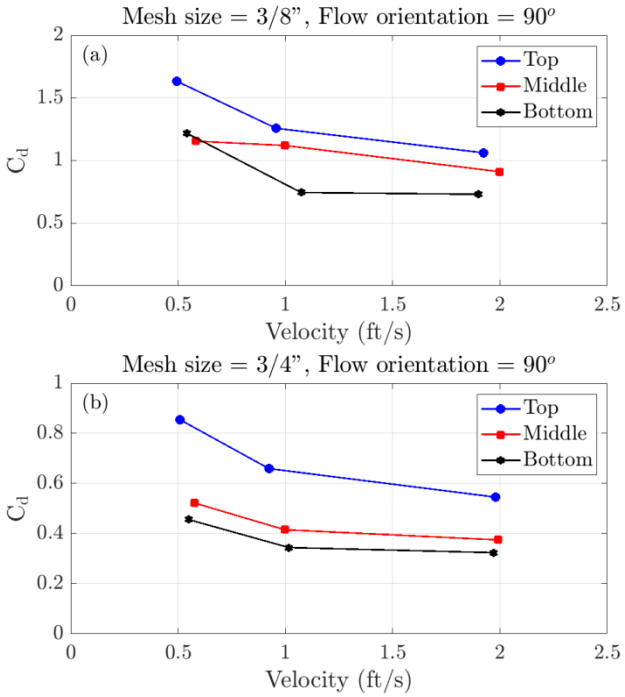

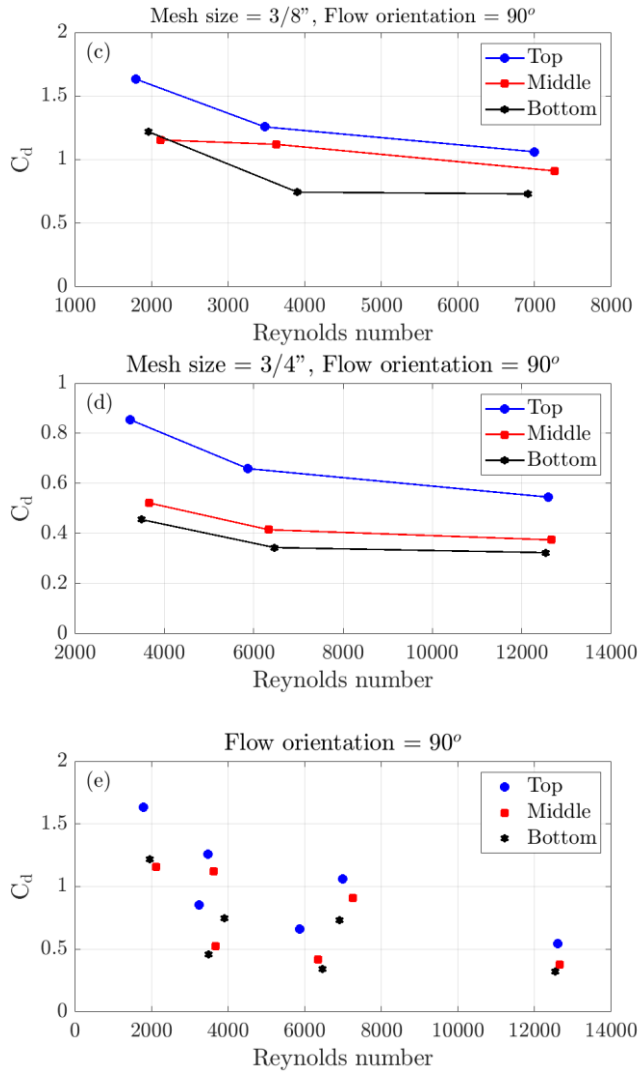

Figure 3-5. The sample nets drag coefficient for 113 days after deployment in water (a) Drag coefficient versus velocity for mesh size 0.375-inch, (b) Drag coefficient versus velocity for mesh size 0.750-inch, (c) Drag coefficient versus Reynolds number for mesh size 0.375-inch, (d) Drag coefficient versus Reynolds number for mesh size 0.750-inch, (e) Drag coefficient versus Reynolds number for mesh size 0.375-inch and 0.750-inch.

3.2 Drag coefficient change in time

As shown in the previous section, the extent of bio-fouling changes the corresponding drag coefficients. This section compares the drag coefficients for different net residence times, for the lowest water approach velocity (Figure 3-6). The highest drag coefficients are observed at day 82 for the top panel (gray circles). These drag coefficients were used in CFD model simulations. Also, the top panel drag coefficient changes more significantly with time as compared to other cases.

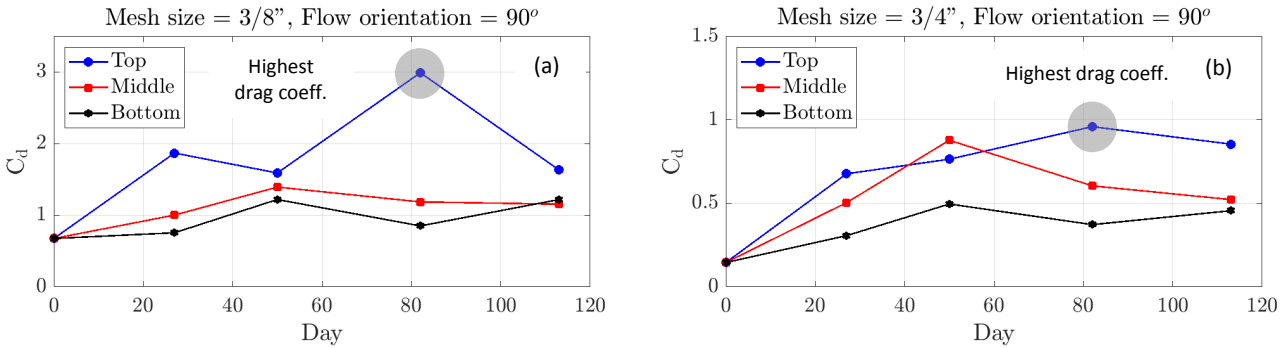

Figure 3-6. (a) Drag coefficient versus time for mesh size 0.375-inch, (b) Drag coefficient versus time for mesh size 0.750-inch.

4.0 CFD Model

4.1 Model Geometry

A FLOW-3D CFD model of the Connecticut River in the vicinity of the Northfield intake/tailwater was previously developed by Alden to evaluate sediment exclusion strategies and is described in detail in Reference 9.0. The CFD model was validated with Acoustic Doppler Current Profiler (ADCP) velocity measurements collected by Gomez and Sullivan directly in the tailrace[1]. The CFD model was modified for the current study to improve the grid resolution in the region of interest around the exclusion net. The channel bathymetry is unchanged from Reference 9.0.

Figure 4-1 shows the four mesh blocks used for the modified CFD model. Mesh Block 1 (in the vicinity of the intake/tailwater) has a resolution of 5 ft in the **X** (north – south) direction, 4 ft in the **Y** (east-west) direction, and 2 ft in the **Z** (depth) direction. Mesh Blocks 2, 3, and 4 have a resolution of 10 ft in the X and Y directions, and 2 ft in the Z direction, which is the vertical direction.

[11] As part of the Federal Energy Regulatory Commission licensing of the Project, Gomez and Sullivan Engineers conducted Study No. 3.3.9 *Two-Dimensional Modeling of the Northfield Mountain Pumped Storage Project Intake/Tailrace Channel and the Connecticut River Upstream and Downstream of the Intake/Tailrace*. As part of that study, velocity was conducted in the tailrace.

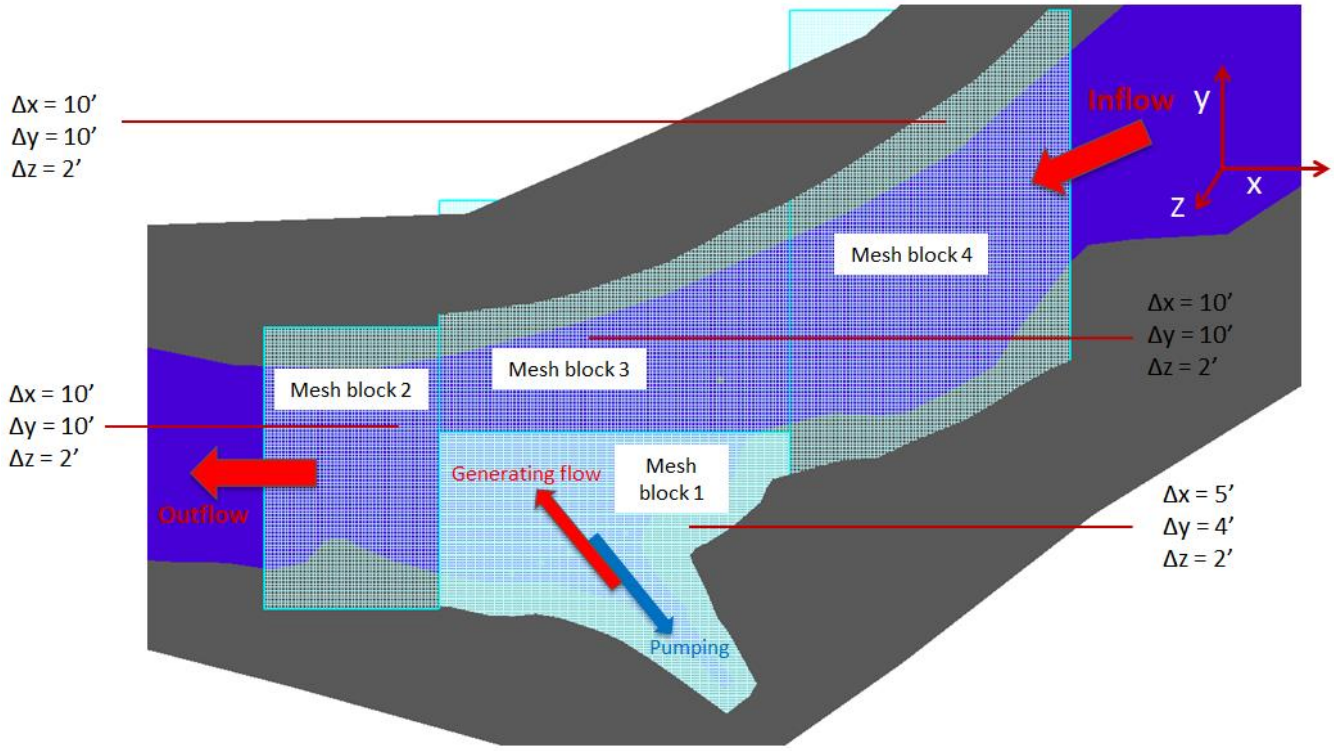

Figure 4-1. CFD model mesh block delineation and boundary conditions.

4.2 Model Boundary Conditions

The flow duration curve for the Connecticut River at Northfield from August 1 to November 15 is shown in Figure 4-2[2]. The Connecticut River flow was higher than 50,000 cfs only 1% of the time within the 2000 to 2010 period of record. River flow exceeds 30,000 cfs 4% of the time and 50% of the time for a river flow of 5,000 cfs.

River conditions that were hypothesized to produce the highest potential velocities through the exclusion net are given in Table 4 1. A low impoundment level minimizes the cross-sectional area through the exclusion net and thereby results in higher velocities through the net. Low, medium, and high Connecticut River flows with corresponding low TFI tailwater levels were selected for the river conditions. Under the current Federal Energy Regulatory Commission (FERC) license for the Project, the lower reservoir (the Turners Falls Impoundment or Connecticut River) can operate between elevations 185 and 176 feet (NGVD29). The river water levels were conservatively selected from the stage-discharge rating curve in Figure 4 3[3]. The stage-discharge rating curve was modified from the annual flow duration curve from Reference 9.0 to only reflect the August 1 to November 15 time

[2] The flow duration curve was computed by subtracting the Millers River from the Naturally Routed Flow calculation (Naturally Route Flow= Vernon discharge + Ashuelot River + Millers River). All flows are based on hourly data.
[3] This plot is based on measured Northfield tailrace elevations under a range of flows.

period. Each river condition was modeled with both the maximum pumping and generation operation. Six total scenarios were tested with the CFD model (Table 4-1).

Table 4-1. River conditions and project operations for model runs.

River Conditions	Case Name	River Flow (cfs)	Water Level at Project Intake/Tailrace (ft)	Pumping Flow (cfs)	Generating Flow (cfs)
High River Flow, Low TFI Level	NorthA1Gen	50,000	185		20,000
High River Flow, Low TFI Level	NorthB1Gen	50,000	185	15,200	
Medium River Flow, Low TFI Level	NorthC1Gen	30,000	182		20,000
Medium River Flow, Low TFI Level	NorthA1Pump	30,000	182	15,200	
Low River Flow, Low TFI Level	NorthB1Pump	5,000	179		20,000
Low River Flow, Low TFI Level	NorthC1Pump	5,000	179	15,200	

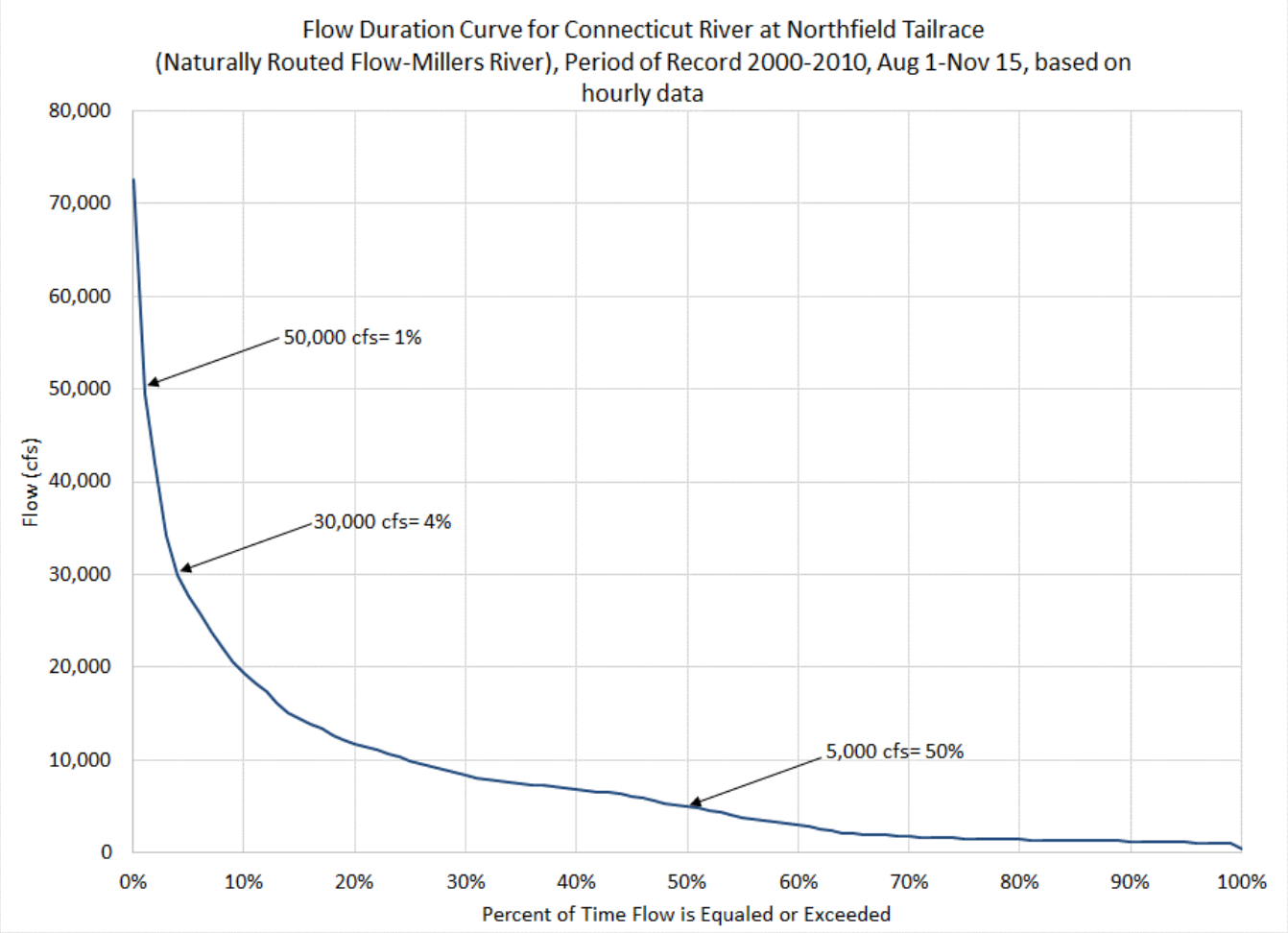

Figure 4-2. Connecticut River flow duration curve at the Northfield Tailrace for August 1 to November 15 (Ref. 9.0).

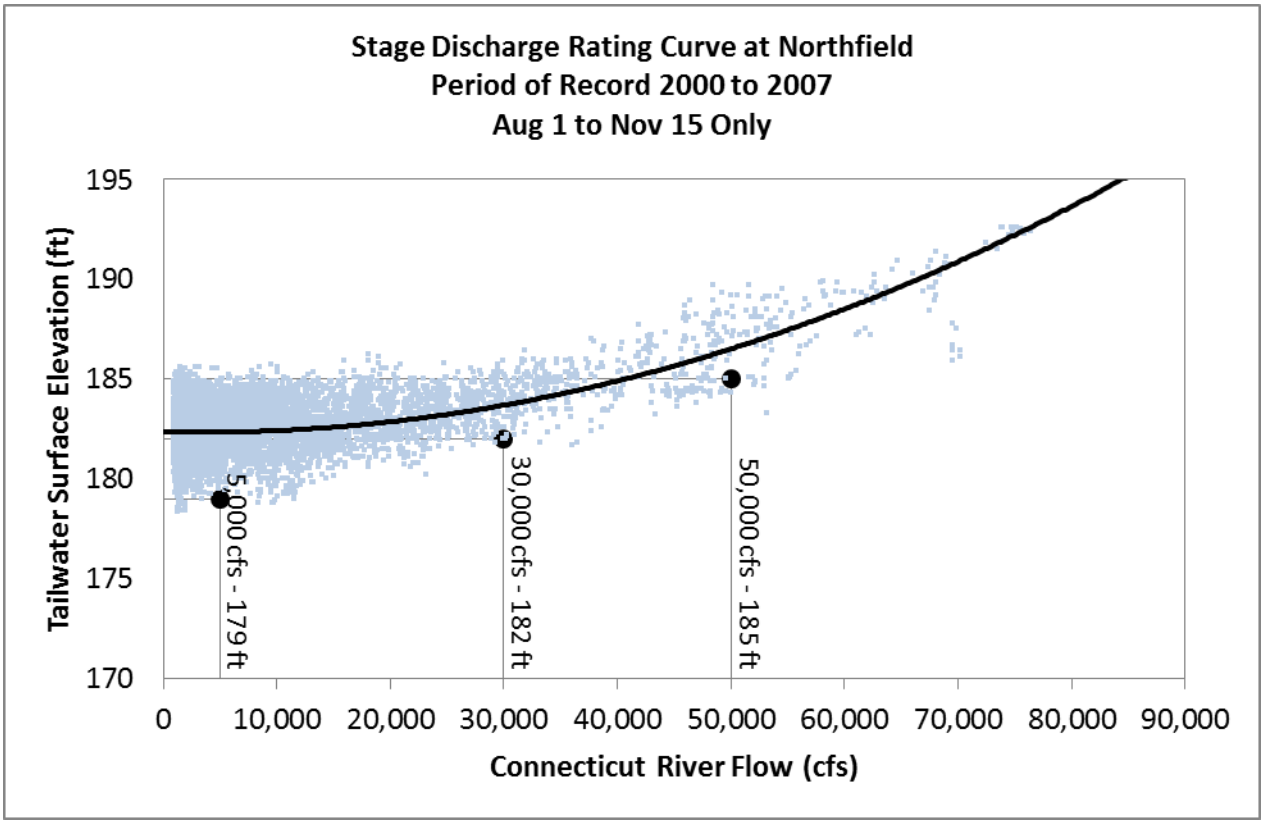

Figure 4-3. Historic stage-discharge relation at Northfield project intake/tailwater.

4.3 Net setup in the model

As mentioned previously, the net was modeled as a porous baffle in FLOW3D. The porosity and the drag coefficient of the net were determined and used as inputs to the model. To assess the maximum possible forces acting on the net, the highest values of drag coefficients obtained from laboratory tests were considered for implementing numerical simulations. The drag coefficient accounts for the bio-fouling and changes in algae growth on the net, as shown in Figure 3-6. However, the porosity of the net is the porosity of a clean net. In order to make the numerical simulation setup as close as possible to the real conditions, simulations similar to laboratory experiments were performed to calibrate the lab-based drag coefficients to be suitable for the main model simulations. The wetted area, head loss, and acting forces on nets were compared with lab results and the drag coefficient was calibrated accordingly. Then, fine-tuned drag coefficients, along with the net porosity (of the clean net), were applied to the two-dimensional porous baffles in the prototype simulations. Hence, while the model is fine tuned to properly model forces, pressure drop, and flow field due to bio-fouling, it does not include the change in porosity caused by bio-fouling. To incorporate the effect of bio-fouling on the mesh size of the net, it is required to directly measure and determine the porosity of the net after the algae growth and use the defined porosity as an input in the numerical model. Therefore, the pore velocity (velocity through the net openings) could be different if the reduction of the mesh size from the bio-fouling could be determined (and hence the fine-tuned drag coefficient used in the model

would also change). However, incorporating the change in pore size due to bio-fouling would not change the flow field and flow direction upstream and downstream of the net, as the acting forces and pressure drops should not change because the drag coefficient is already fine-tuned such that to correctly capture these quantities.

5.0 Force Calculations

The normal and tangential forces acting on the exclusion net were calculated by performing CFD simulations with FLOW-3D. The simulations were performed until a steady state solution was reached. The exclusion net is approximately 30 ft tall (varies with depth) and two panels in the vertical direction that are each approximately 15 ft tall. In the model, a porous baffle was used to simulate the exclusion net, which is taut and occupies a flat vertical plane. In reality, the exclusion net would bow and ripple with the current and not be perfectly vertical. It was assumed that the top panel was always taut and 15 ft deep. The lower panel extends from the base of the top panel at the 15 ft depth to the river bottom bathymetry. For this study, two main cases are considered: 1) Generation case; and 2) Pumping case.

5.1 Generation case

Three cases for the generation scenario were considered:

1) Generation flow rate = 20,000 cfs and river flow rate = 50,000 cfs (high river flow rate);

2) Generation flow rate = 20,000 cfs and river flow rate = 30,000 cfs (medium river flow rate); and

3) Generation flow rate = 20,000 cfs and river flow rate = 5,000 (low river flow rate).

Velocity distribution near the exclusion net is also illustrated. A complete summary of the force and average velocity at each net is presented in Appendix A.

5.1.1 Force calculation

Figure 5-1 shows forces for the generation case with the flow rate = 20,000 cfs and the river flow rate = 50,000 cfs, Figure 5-2 is the generation case with the flow rate = 20,000 cfs and the river flow rate = 30,000 cfs and Figure 5-3 illustrates the generation case with the flow rate = 20,000 cfs and the river flow rate = 5,000 cfs. In these figures, the normal and tangential forces (panel a) and flow through both nets and each individual net are illustrated (panel b). The simulations were implemented until the steady state was obtained (flat part of the curves in panels a and b). The results in panels (b) show that the total flow through the net is very close to the flow rate released from the reservoir at the upstream (20,000 cfs). Also, the normal force increases with the decrease of the river flow rate (~40,500 lb for the river flow rate = 50,000 cfs, ~52,000 lb for the river flow rate = 30,000 cfs, and ~60,000 lb for the river flow rate = 5,000 cfs). On the other side, the tangential forces are not considerably different from each other (~5,900 lb for the river flow rate = 50,000 cfs, ~6,300 lb for the river flow rate = 30,000 cfs, and 4,700 lb for the river flow rate = 5,000 cfs). A summary of the force results is shown in Table 5-1.

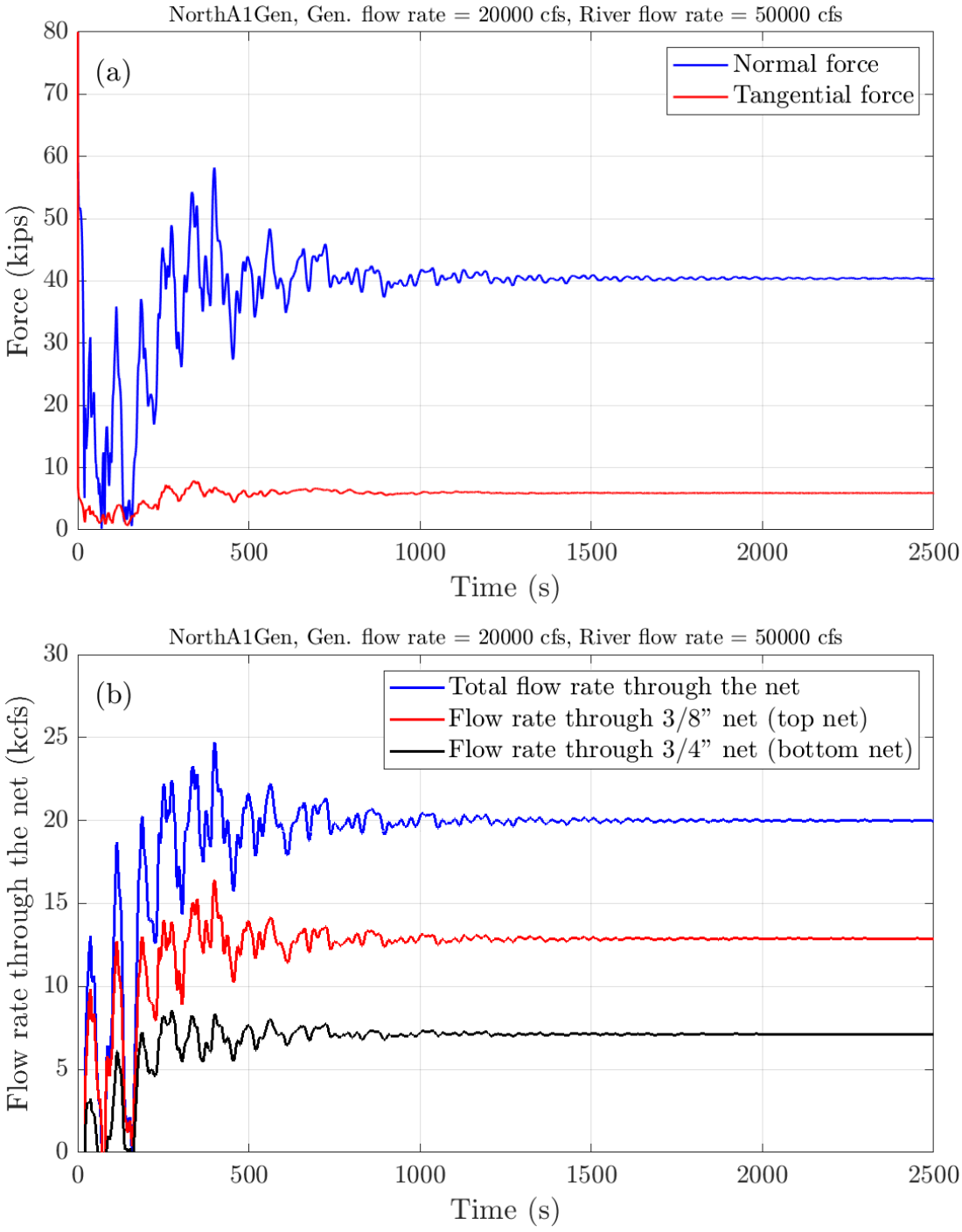

Figure 5-1. (a) The normal and tangential forces on the nets for the generation case with flow rate = 20,000 cfs, river flow rate = 50,000 cfs, and water level 185 ft, (b) Total flow rate and the flow rate through the top and bottom nets (mesh size 0.375-inch and 0.750-inch, respectively).

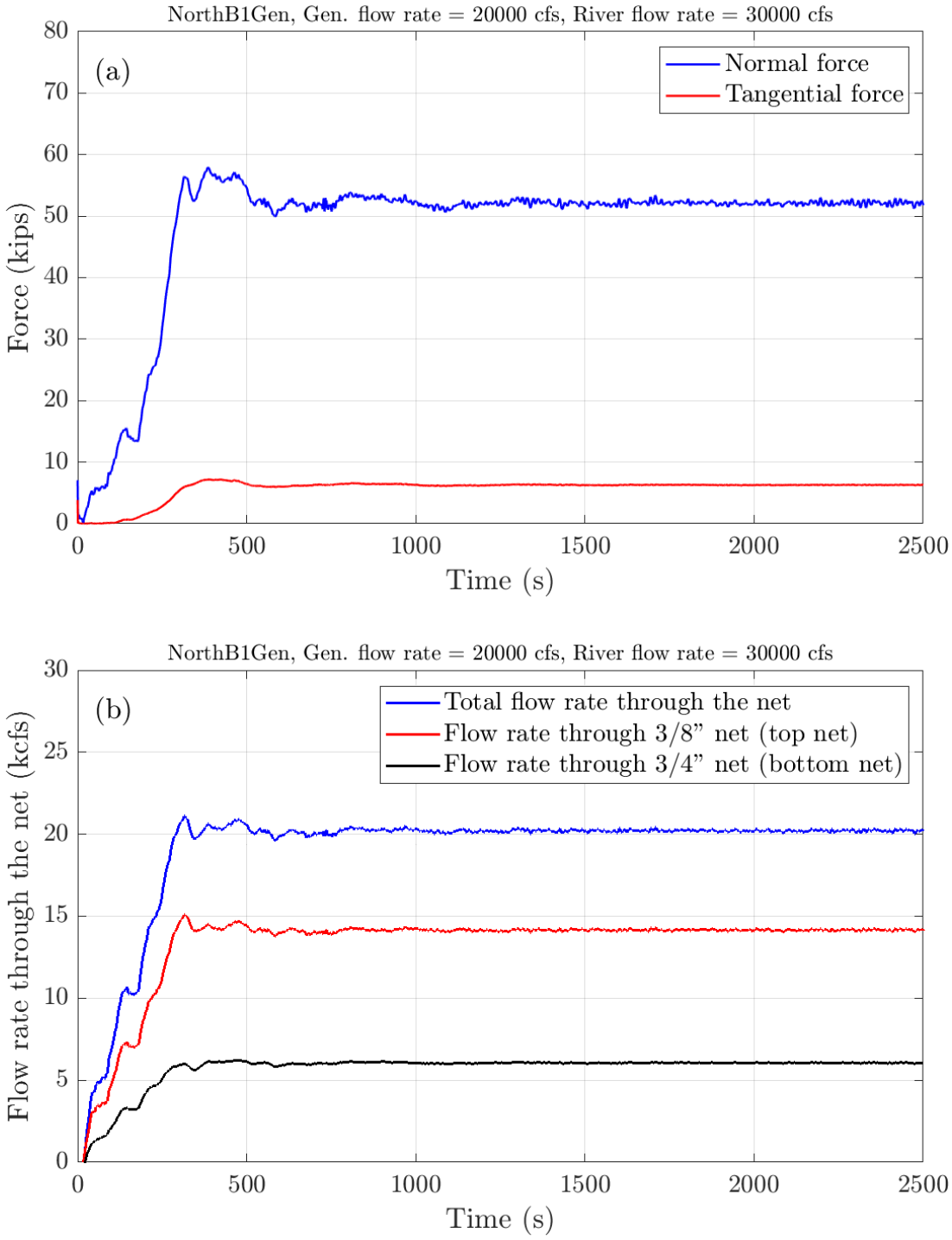

Figure 5-2. The normal and tangential forces on the nets for the generation case with flow rate = 20,000 cfs, river flow rate = 30,000 cfs, and water level 182 ft, (b) Total flow rate and the flow rate through the top and bottom nets (mesh size 0.375-inch and 0.750-inch, respectively).

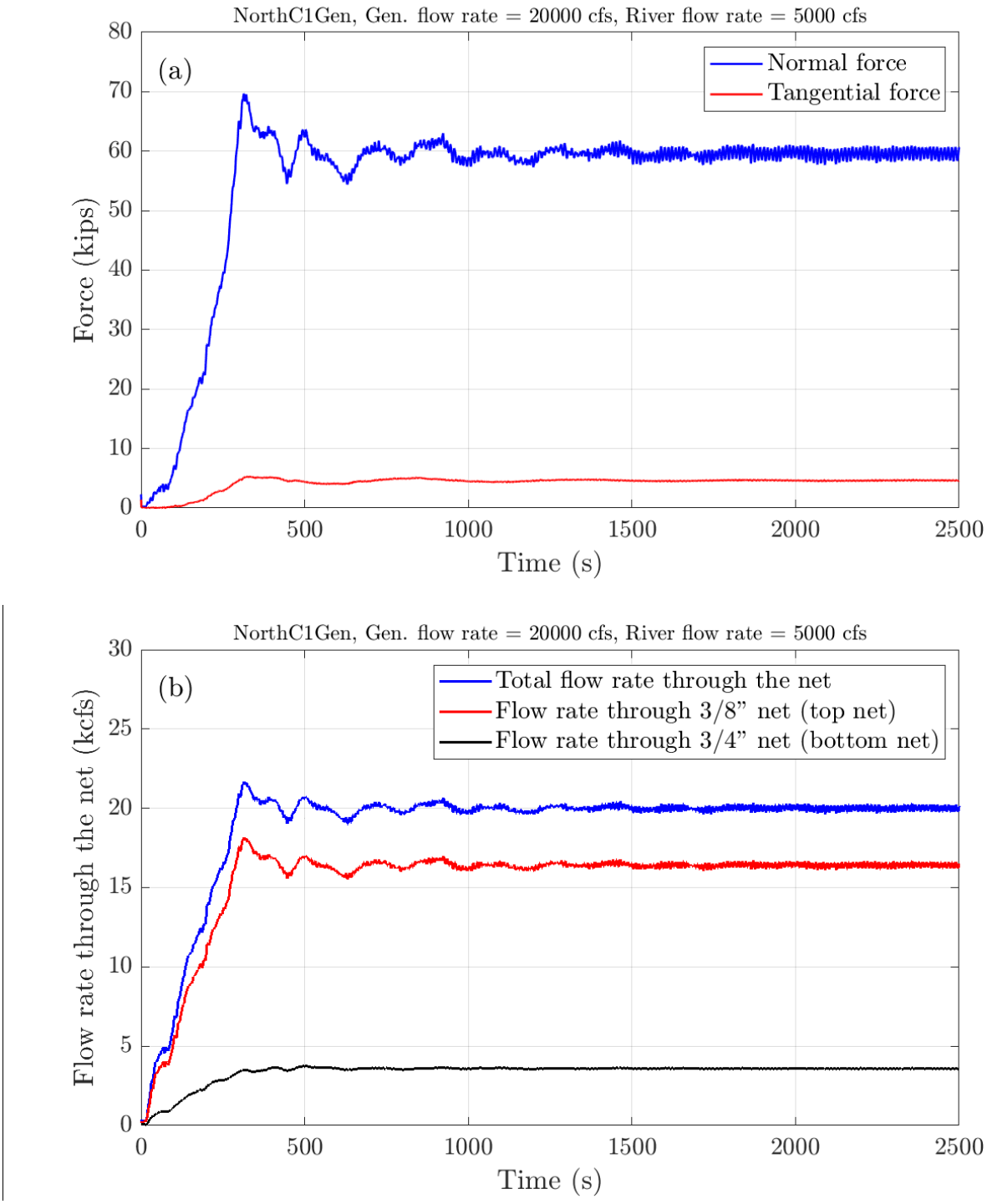

Figure 5-3. (a) The normal and tangential forces on the nets for the generation case with flow rate = 20,000 cfs, river flow rate = 5,000 cfs, and water level 179 ft, (b) Total flow rate and the flow rate through the top and bottom nets (mesh size 0.375-inch and 0.750-inch, respectively).

Table 5-1. Summary of the generation flow.

River cond.	River flow (cfs)	Water lev. Intake/Tailrace (ft)	Gen. flow (cfs)	Total area (ft^2)	Norm. force (lb)	Tang. force (lb)	Avg. Norm. force per unit area (lb/ft^2)
High flow	50,000	185	20,000	24,871	40,500	5,900	1.63
Med. flow	30,000	182	20,000	21,236	52,000	6,300	2.45
Low flow	5,000	179	20,000	17,215	60,000	4,700	3.49

5.1.2 Velocity distribution

Velocity distribution near the net is illustrated in both horizontal and vertical planes. Figures 5-4 and 5-5 show the horizontal velocity distribution in the horizontal and vertical planes for the generation case with flow rate = 20,000 cfs and river flow rate = 50,000 cfs. Figures 5-6 and 5-7 illustrate the horizontal velocity distribution in the horizontal and vertical planes for the generation case with flow rate = 20,000 cfs and river flow rate = 30,000 cfs. Finally, Figures 5-8 and 5-9 show the horizontal velocity distribution in the horizontal and vertical planes for the generation case with flow rate = 20,000 cfs and the low river flow rate = 5,000 cfs. In these figures, the arrows are showing the horizontal velocity vectors.

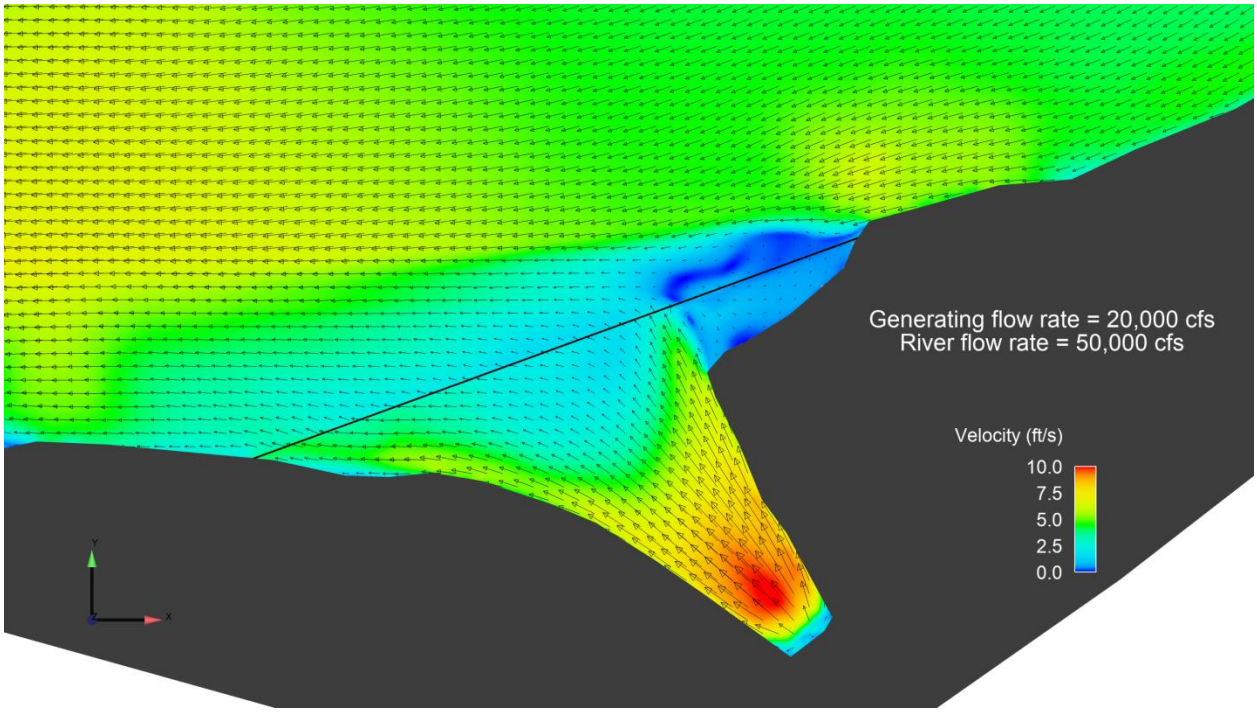

Figure 5-4. The horizontal velocity distribution for the generation case at $z = 183$ ft with flow rate = 20,000 cfs, river flow rate = 50,000 cfs, and water level 185 ft.

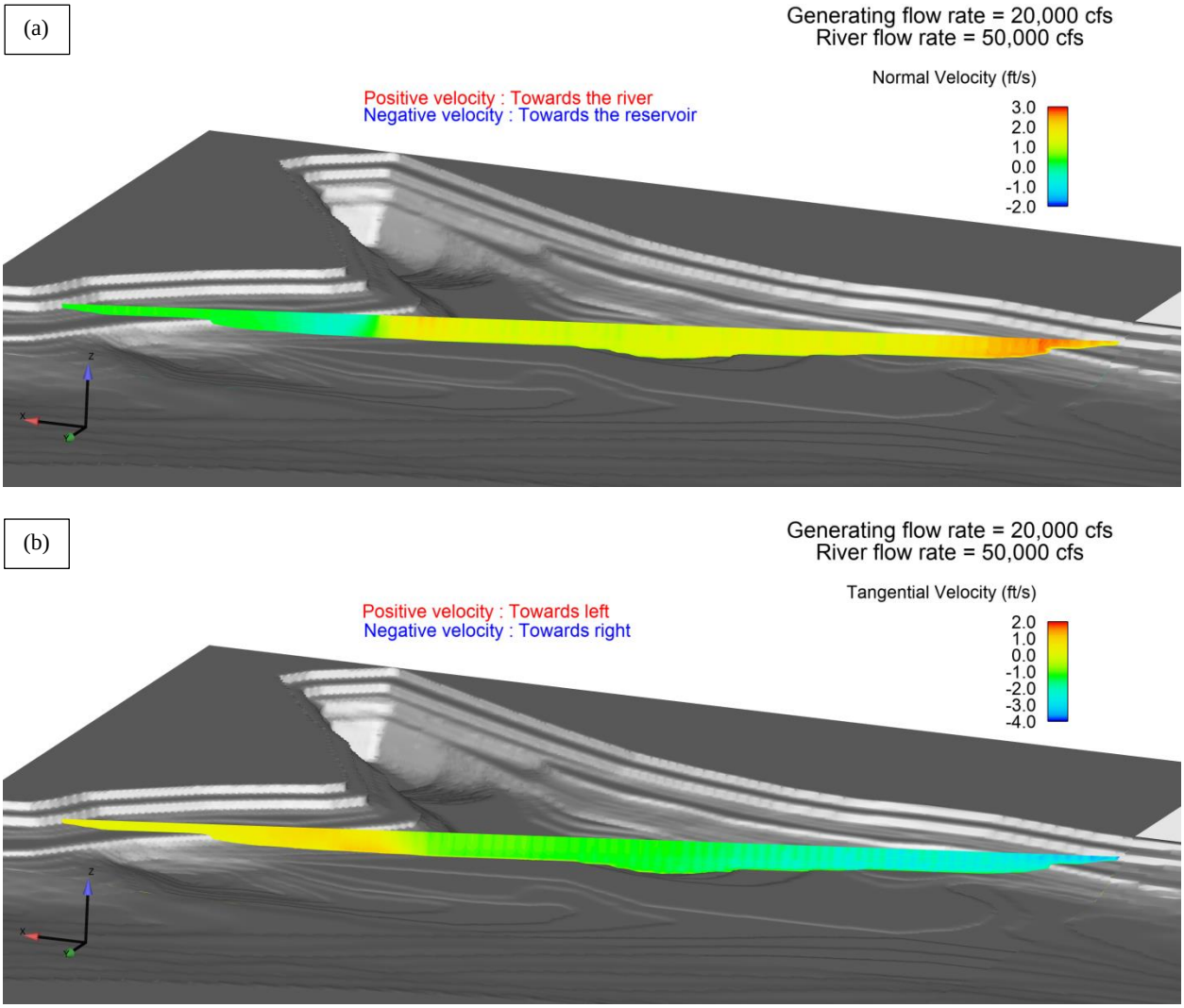

Figure 5-5. (a) The normal velocity, and (b) the tangential velocity; for the generation case about 1 ft upstream of the net (side of the reservoir) with generation flow rate = 20,000 cfs, river flow rate = 50,000 cfs, and water level 185 ft.

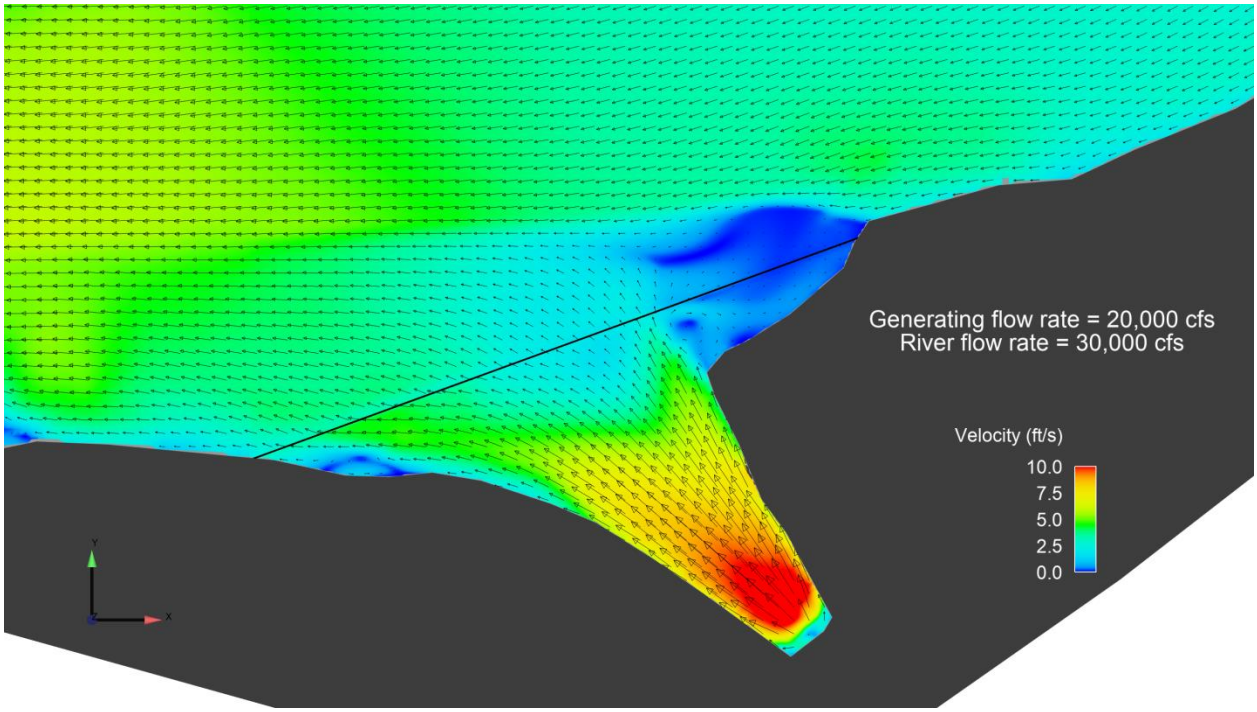

Figure 5-6. The horizontal velocity distribution for the generation case at $z = 182$ ft with generation flow rate = 20,000 cfs, river flow rate = 50,000 cfs, and water level 182 ft.

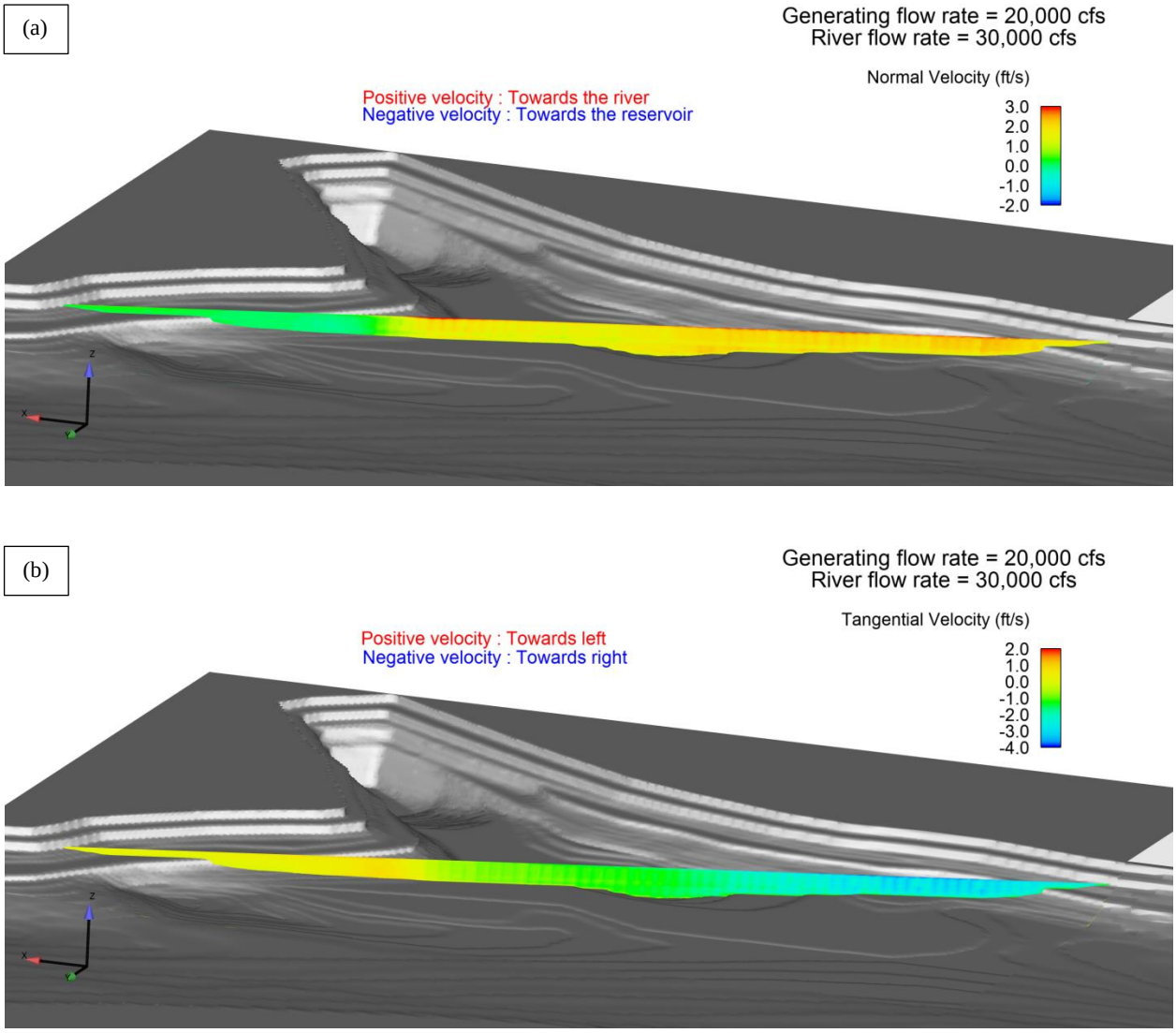

Figure 5-7. (a) The normal velocity, and (b) the tangential velocity; for the generation case about 1 ft upstream of the net (side of the reservoir) with generation flow rate = 20,000 cfs, river flow rate = 30,000 cfs, and water level 182 ft.

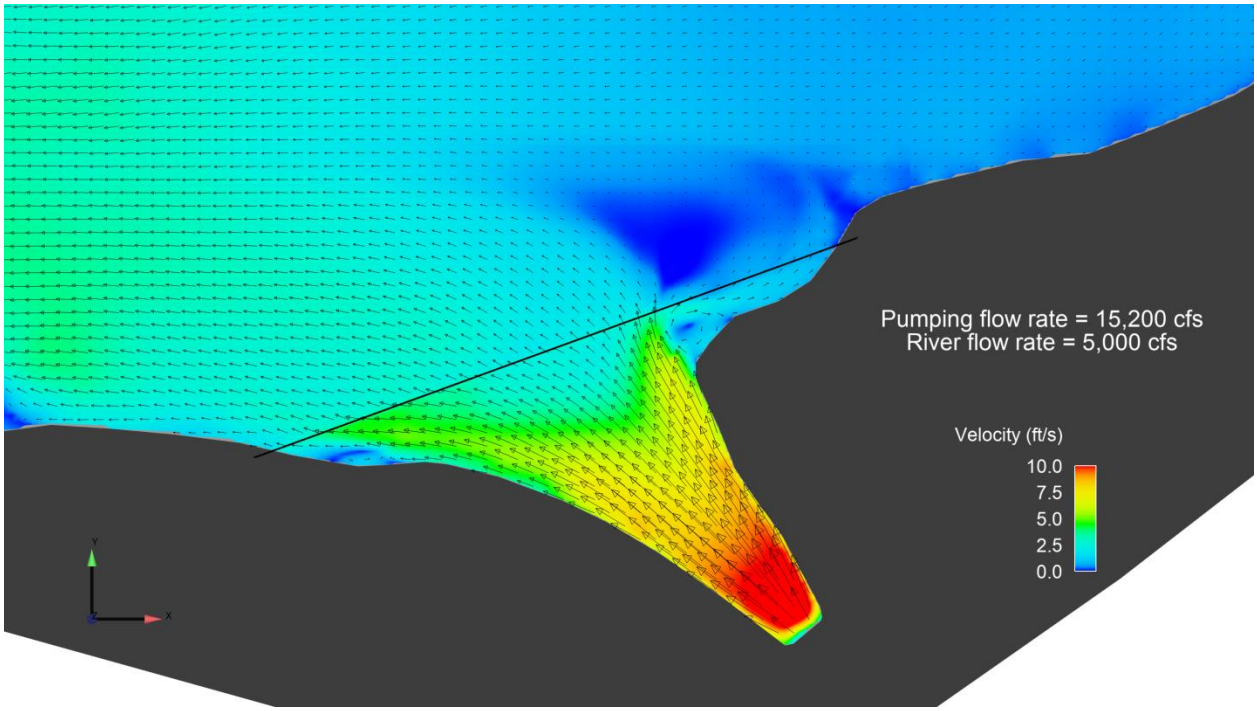

Figure 5-8. The horizontal velocity distribution for the generation case at $z = 178$ ft with generation flow rate = 20,000 cfs, river flow rate = 5,000 cfs, and water level 179 ft.

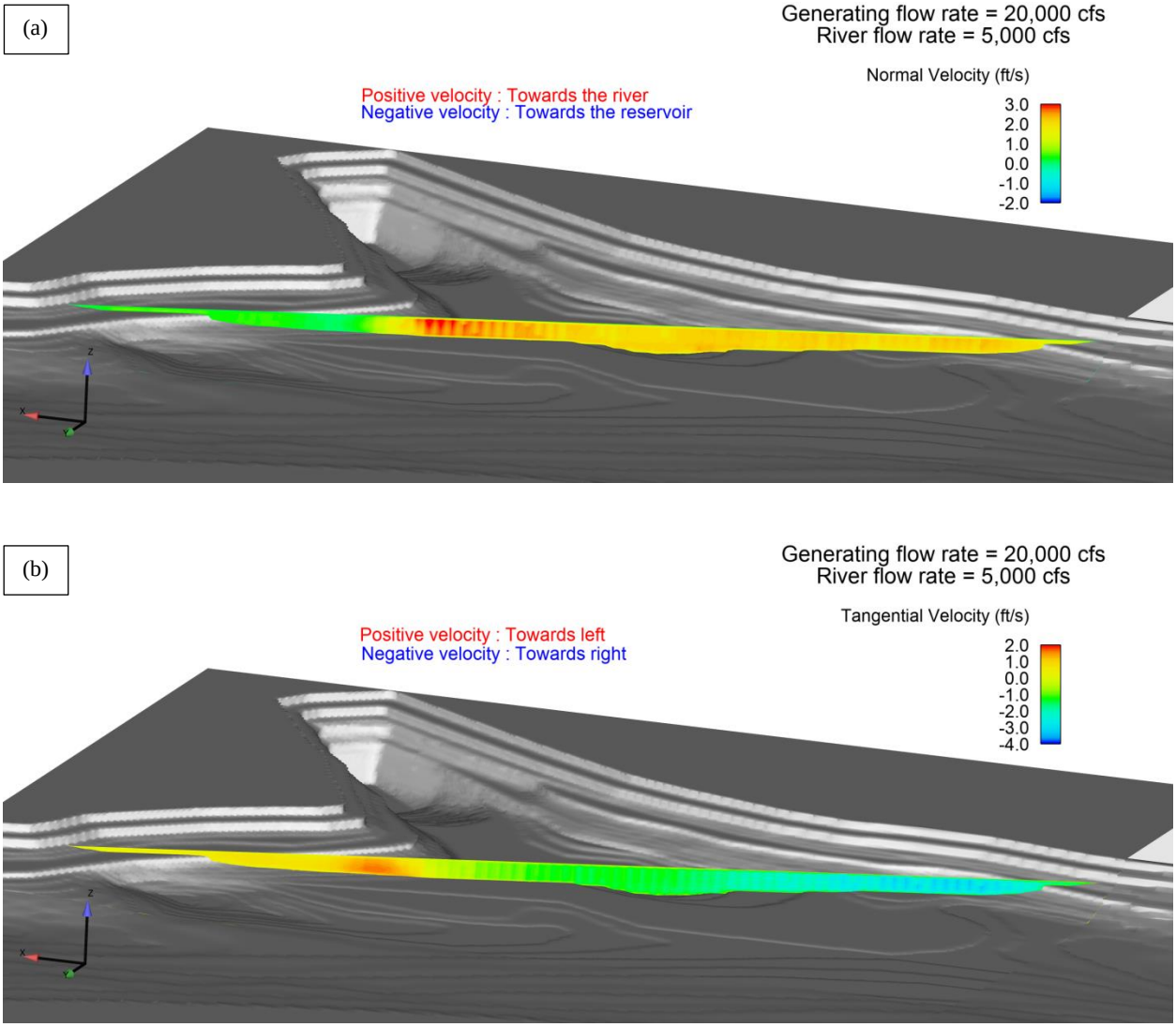

Figure 5-9. (a) The normal velocity, and (b) the tangential velocity; for the generation case about 1 ft upstream of the net (side of the reservoir) with generation flow rate = 20,000 cfs, river flow rate = 5,000 cfs, and water level 179 ft.

5.2 Pumping case

Three cases for the pumping scenario were considered: 1) Pumping flow rate = 15,200 cfs and river flow rate = 50,000 cfs (high river flow rate); 2) Pumping flow rate = 15,200 cfs and river flow rate = 30,000 cfs (medium river flow rate); and 3) Pumping flow rate = 15,200 cfs and river flow rate = 5,000 (low river flow rate). Similar to the generation case, in this section the normal and tangential forces, flow through both nets and each individual net and velocity distribution are illustrated. A complete summary of the force and average velocity at each net is presented in Appendix A.

5.2.1 Force calculation

Figure 5-10 shows forces for the pumping case with the pumping flow rate = 15,200 cfs and river flow rate = 50,000 cfs, Figure 5-11 is for the pumping case with the pumping flow rate = 15,200 cfs and river flow rate = 30,000 cfs and Figure 5-12 illustrates the pumping case with the pumping flow rate = 15,200 cfs and river flow rate = 5,000 cfs. In these figures, the normal and tangential forces (panel a) and flow through both nets and each individual net are illustrated (panel b). The simulations were implemented until a steady state solution was obtained (flat part of the line in panels a and b). Again, the results in panels (b) show that the total flow through the net is very close to the flow rate pumped from the river (15,200 cfs). Also, the normal forces are ~40,000 lb for the river flow rate = 50,000 cfs, ~45,000 lb for the river flow rate = 30,000 cfs, and ~32,500 lb for the river flow rate = 5,000 cfs. The tangential forces are ~3,800 lb for the river flow rate = 50,000 cfs, ~3,100 lb for the river flow rate = 30,000 cfs, and 600 lb for the river flow rate = 5,000. A summary of the force and velocity results is shown in Table 5-2.

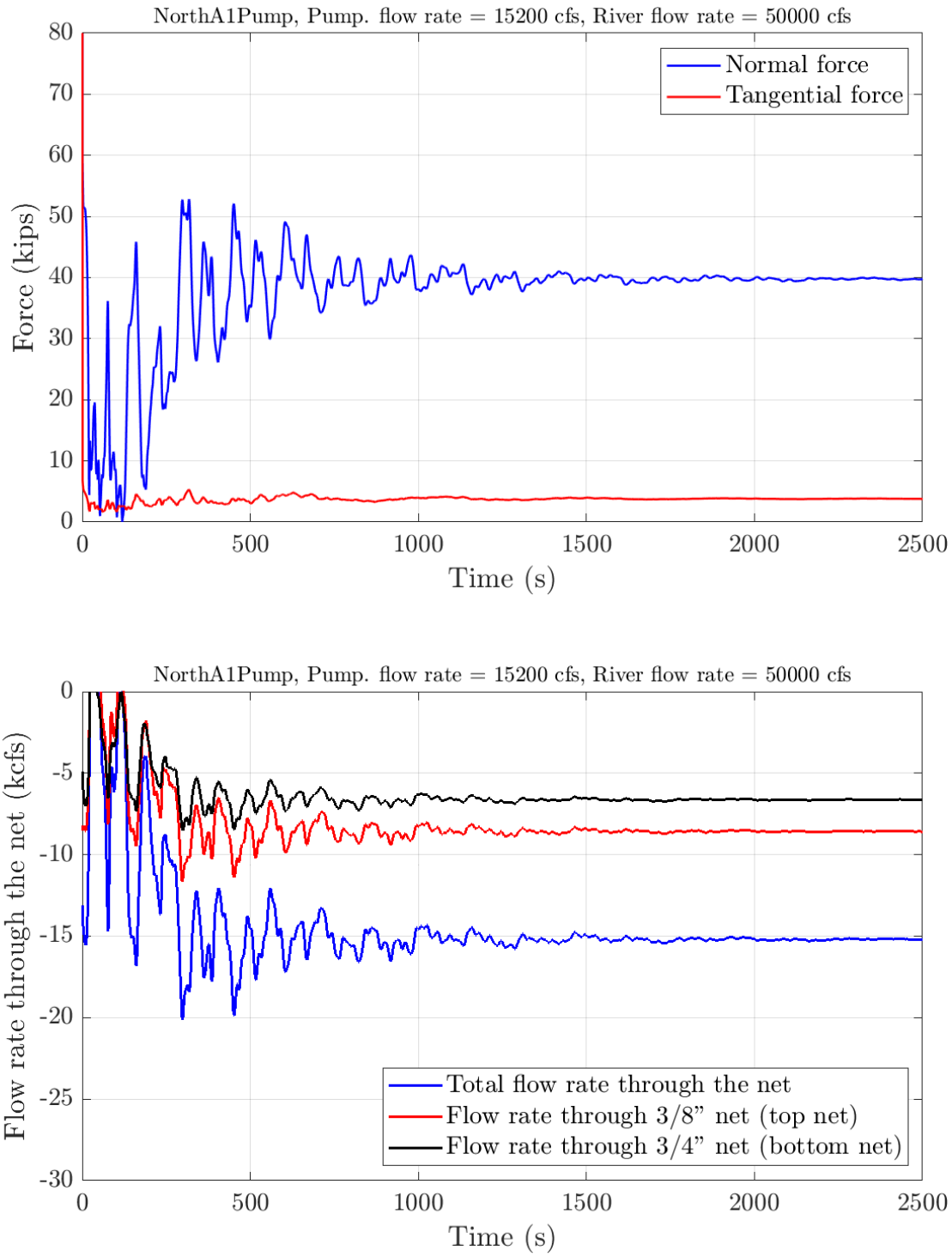

Figure 5-10. (a) The normal and tangential forces on the nets for the pumping case with flow rate = 15,200 cfs, river flow rate = 50,000 cfs, and water level 185 ft, (b) Total flow rate and the flow rate through the top and bottom nets (mesh size 0.375-inch and 0.750-inch, respectively).

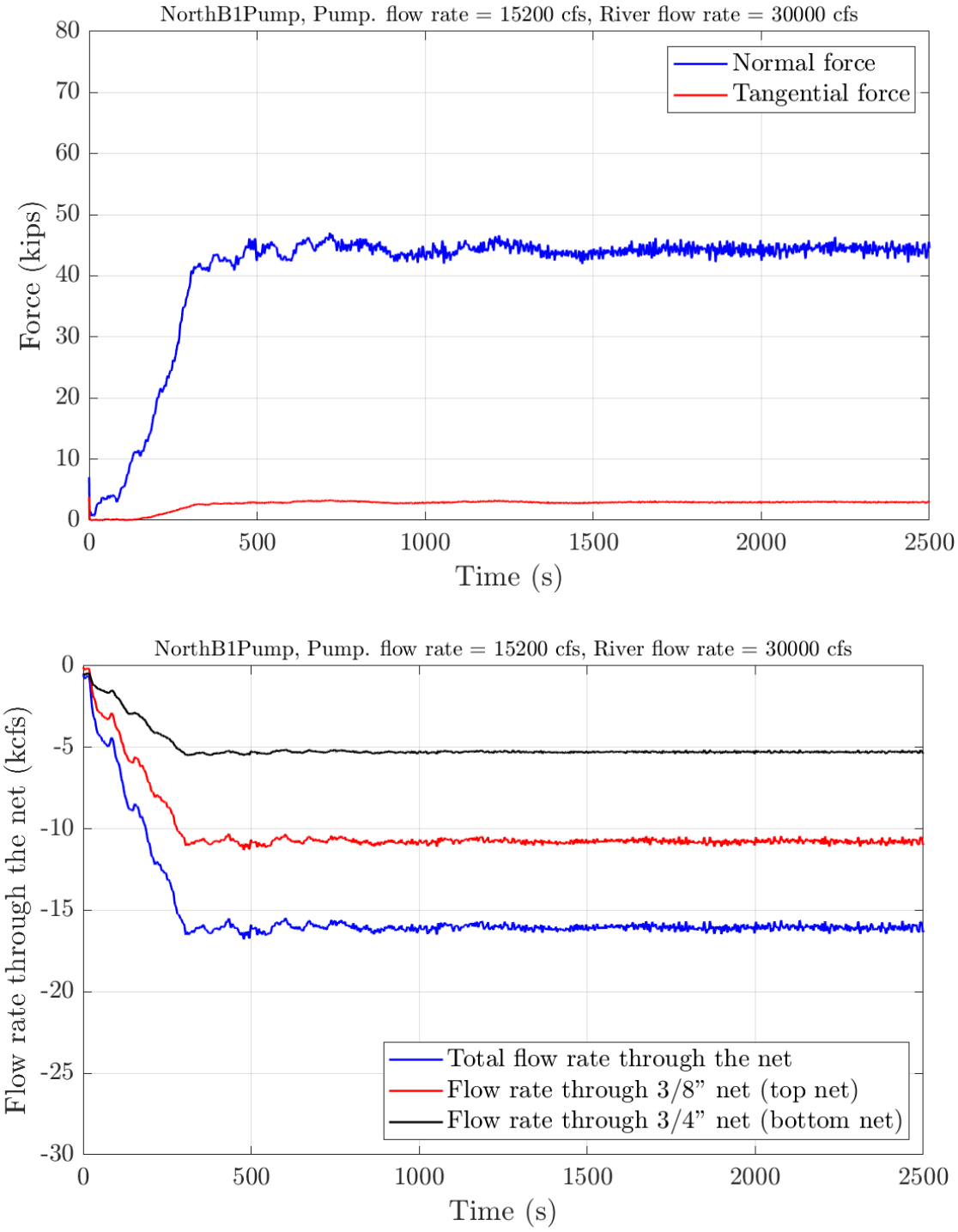

Figure 5-11. (a) The normal and tangential forces on the nets for the pumping case with flow rate = 15,200 cfs, river flow rate = 30,000 cfs, and water level 182 ft, (b) Total flow rate and the flow rate through the top and bottom nets (mesh size 0.375-inch and 0.750-inch, respectively).

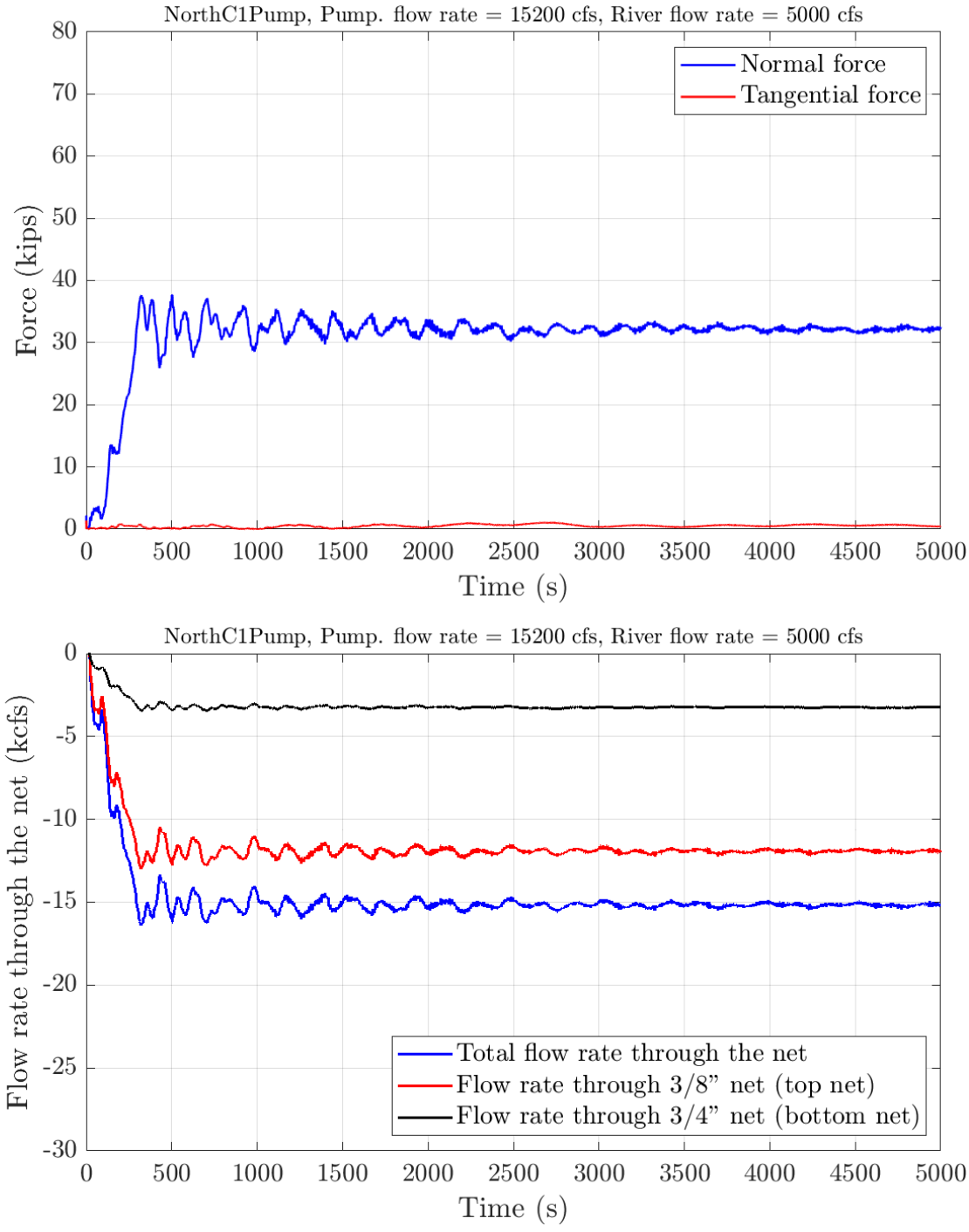

Figure 5-12. (a) The normal and tangential forces on the nets for pumping case with flow rate = 15,200 cfs, river flow rate = 5,000 cfs, and water level 179 ft, (b) Total flow rate and the flow rate through the top and bottom nets (mesh size 0.375-inch and 0.750-inch, respectively).

Table 5-2. Summary of the pumping flow.

River cond.	River flow (cfs)	Water lev. Intake/Tailrace (ft)	Pump. flow (cfs)	Total area (ft^2)	Norm. force (lb)	Tang. force (lb)	Avg. Norm. force per unit area (lb/ft^2)
High flow	50,000	185	15,200	24,361	40,000	3,800	1.64
Med. flow	30,000	182	15,200	21,170	45,000	3,100	2.13
Low flow	5,000	179	15,200	16,998	32,500	600	1.91

5.2.2 Velocity distribution

Velocity distribution near the net is illustrated in both horizontal and vertical planes. Figures 5-13 andFigure 5-14 show the horizontal velocity distribution in the horizontal and vertical planes for the pumping case with flow rate = 15,200 cfs and river flow rate = 50,000 cfs. Figures Figure 5-15 and Figure 5-16 illustrate the horizontal velocity distribution in the horizontal and vertical planes for the pumping case with flow rate = 15,200 cfs and river flow rate = 30,000 cfs. Figures 5-17 and 5-18 show the horizontal velocity distribution in the horizontal and vertical planes for the pumping case with flow rate = 15,200 cfs and river flow rate = 5,000 cfs.

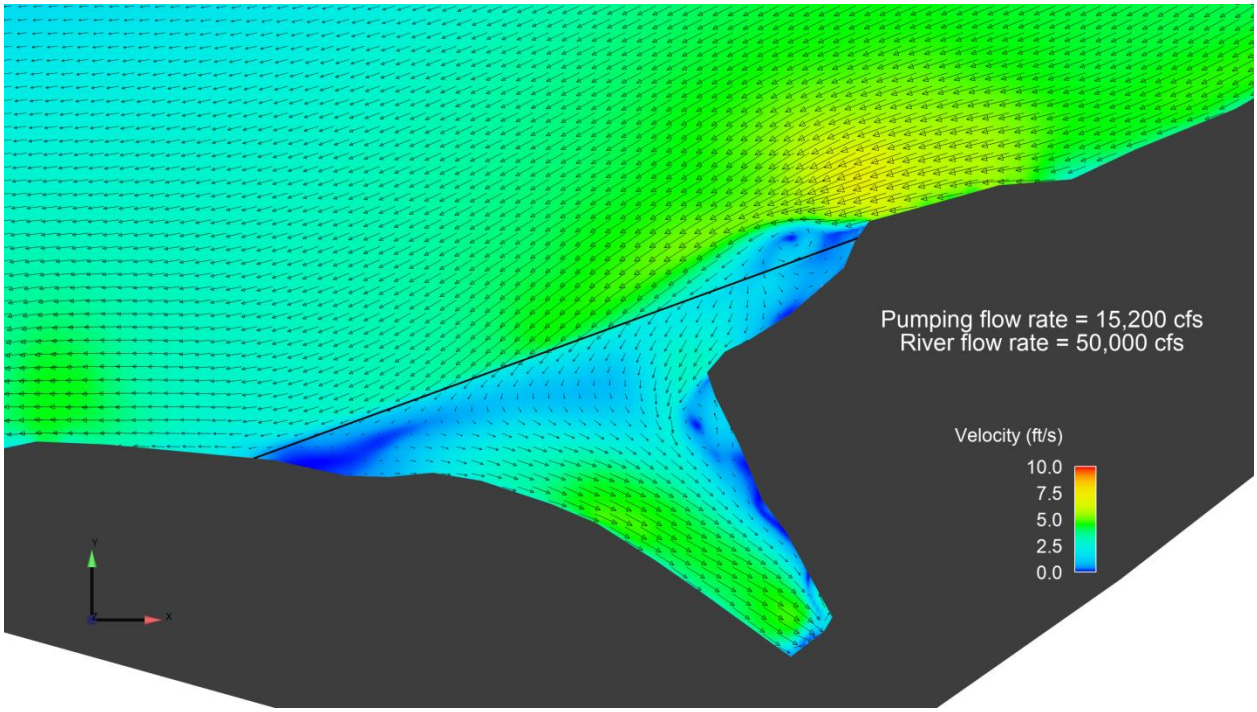

Figure 5-13. The horizontal velocity distribution for the pumping case at $z = 183$ ft with flow rate = 15,200 cfs, river flow rate = 50,000 cfs, and water level 185 ft.

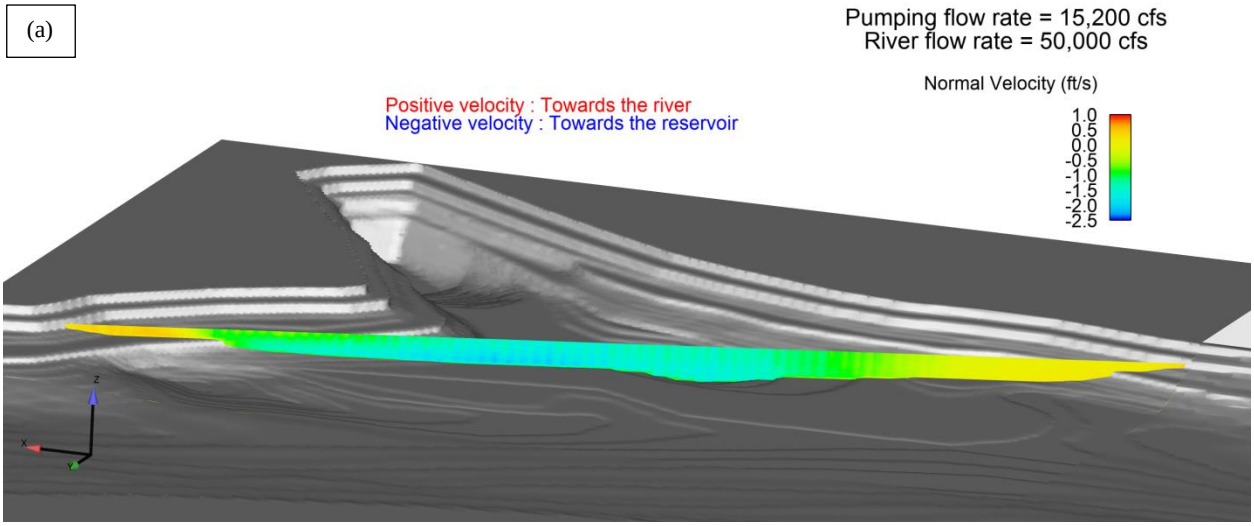

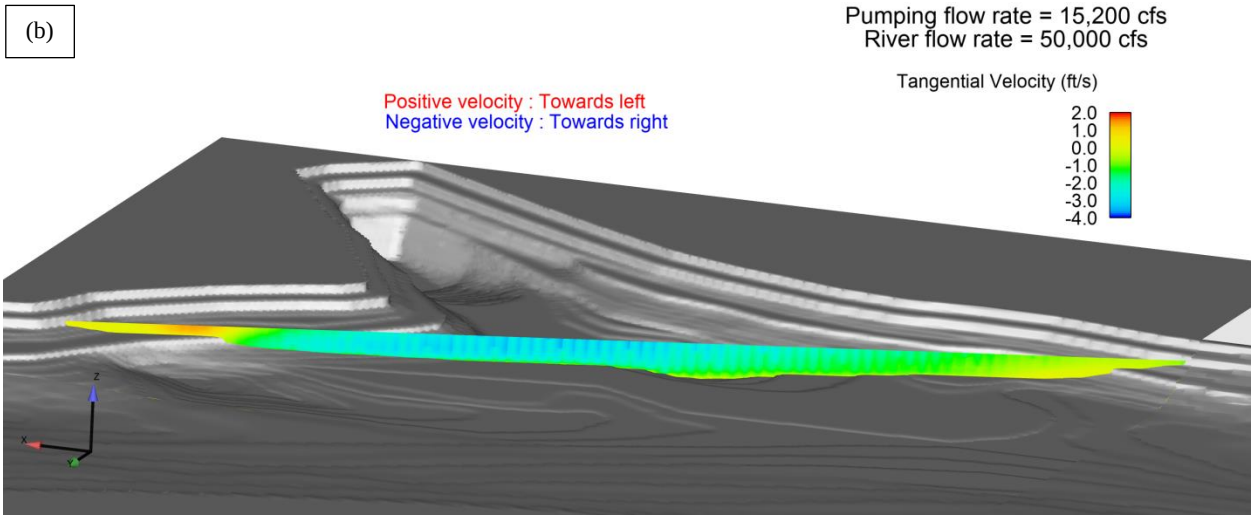

Figure 5-14. (a) The normal velocity, and (b) the tangential velocity; for the pumping case about 1 ft upstream of the net (side of the river) with flow rate = 15,200 cfs, river flow rate = 50,000 cfs, and water level 185 ft.

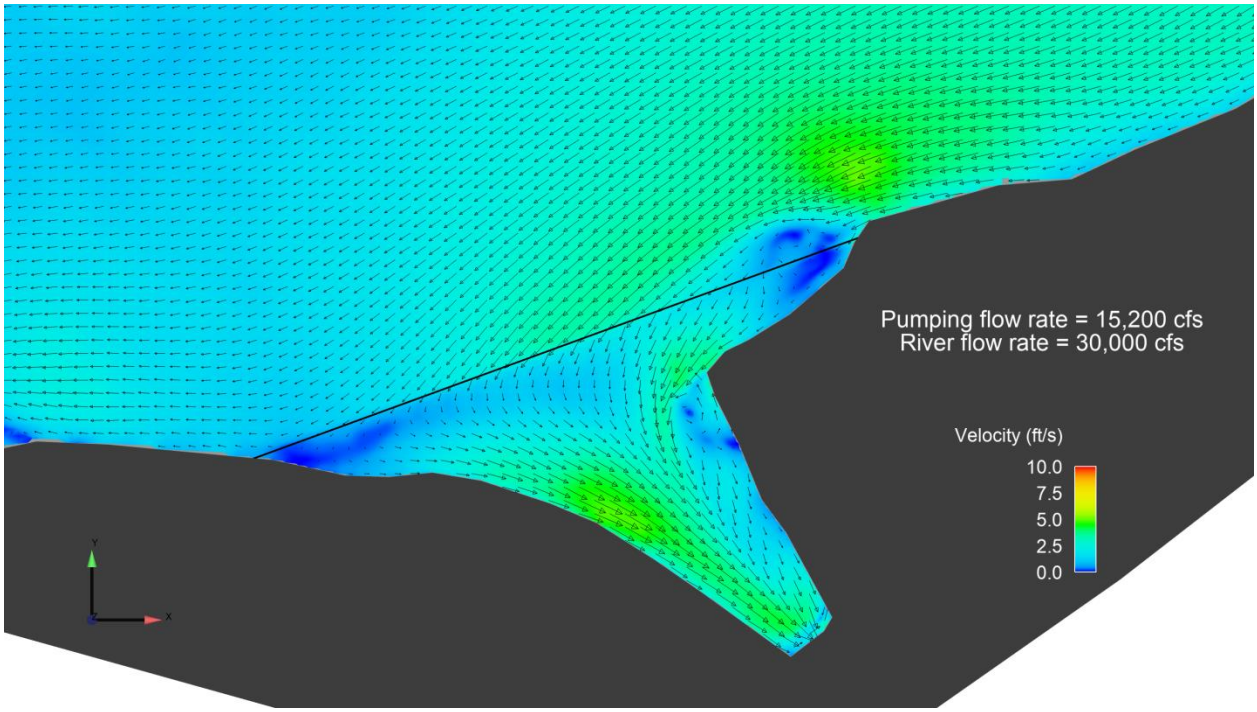

Figure 5-15. The horizontal velocity distribution for the pumping case at $z = 182$ ft with flow rate = 15,200 cfs, river flow rate = 30,000 cfs, and water level 182 ft.

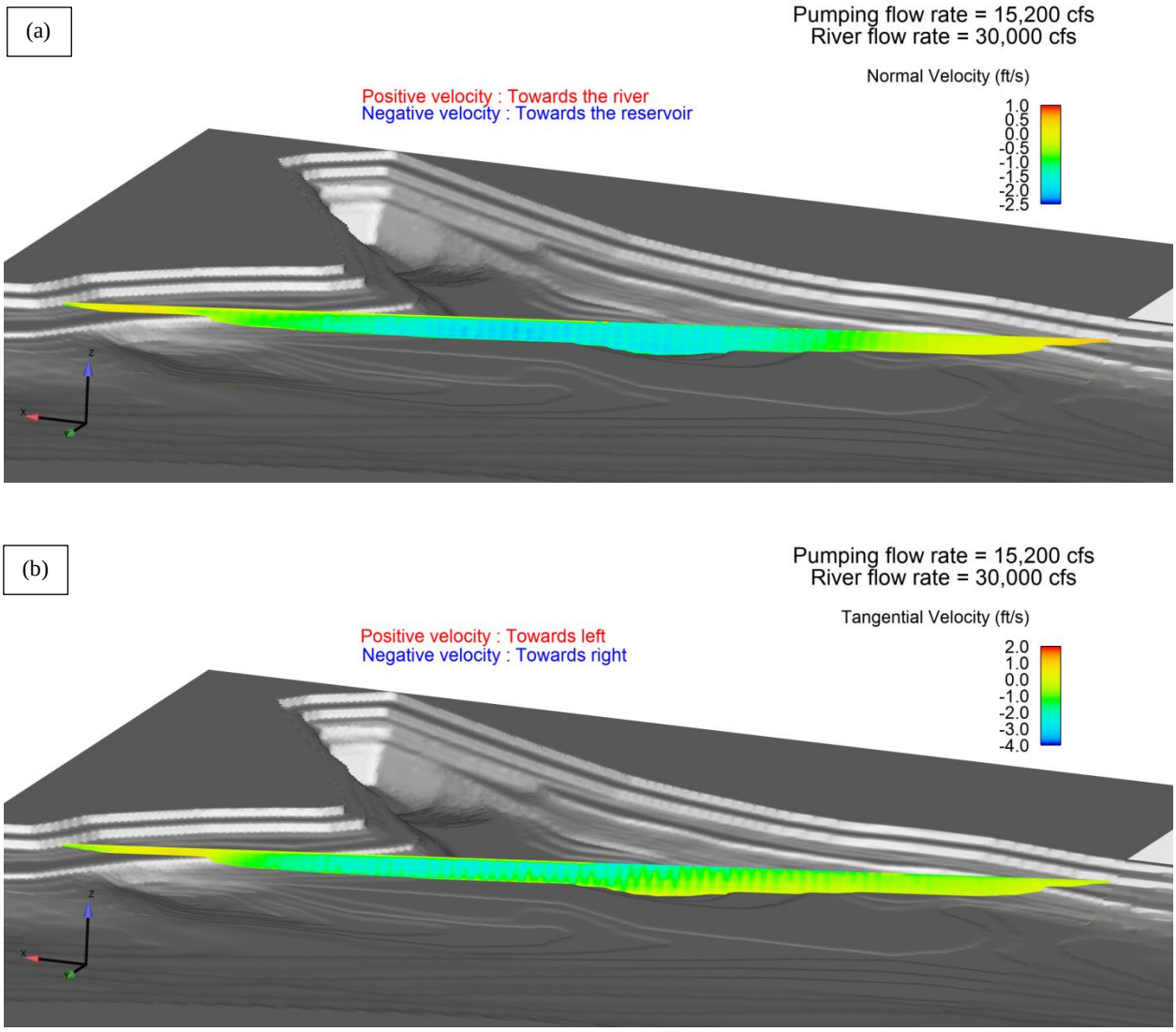

Figure 5-16. (a) The normal velocity, and (b) the tangential velocity; for the pumping case about 1 ft upstream of the net (side of the river) with flow rate = 15,200 cfs, river flow rate = 30,000 cfs, and water level 182 ft.

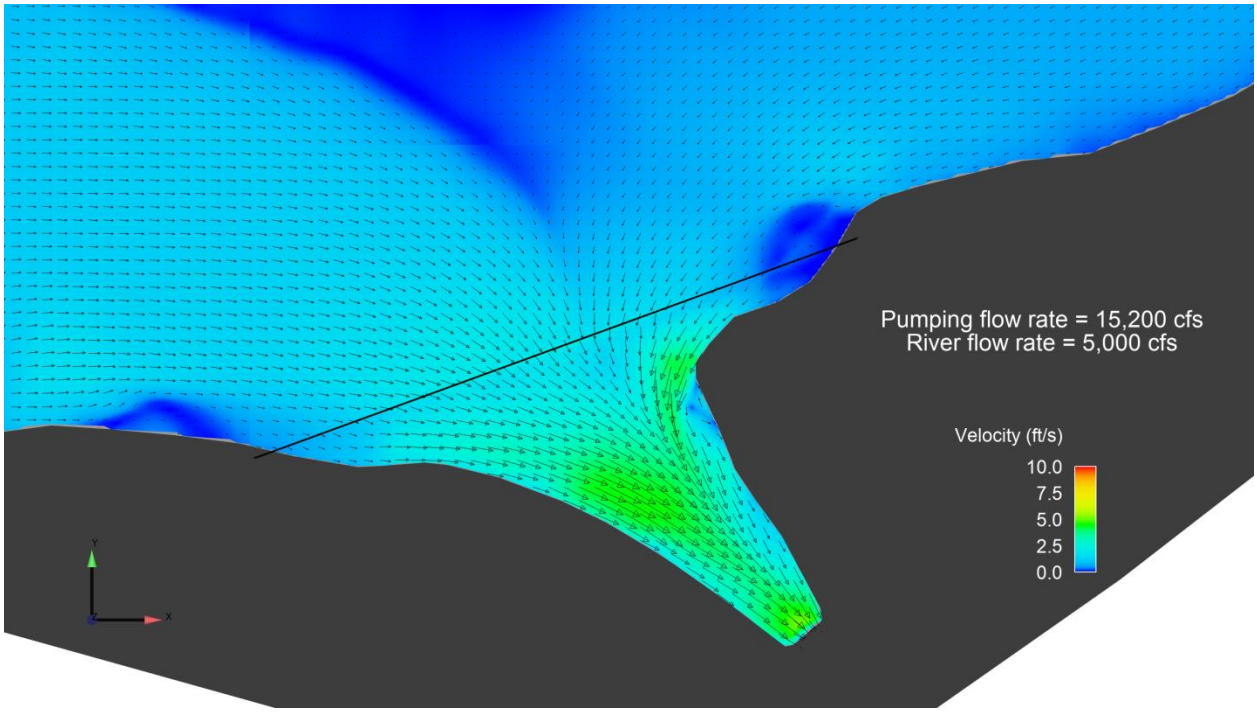

Figure 5-17. The horizontal velocity distribution for the pumping case at $z = 178$ ft with flow rate = 15,200 cfs, river flow rate = 5,000 cfs, and water level 179 ft.

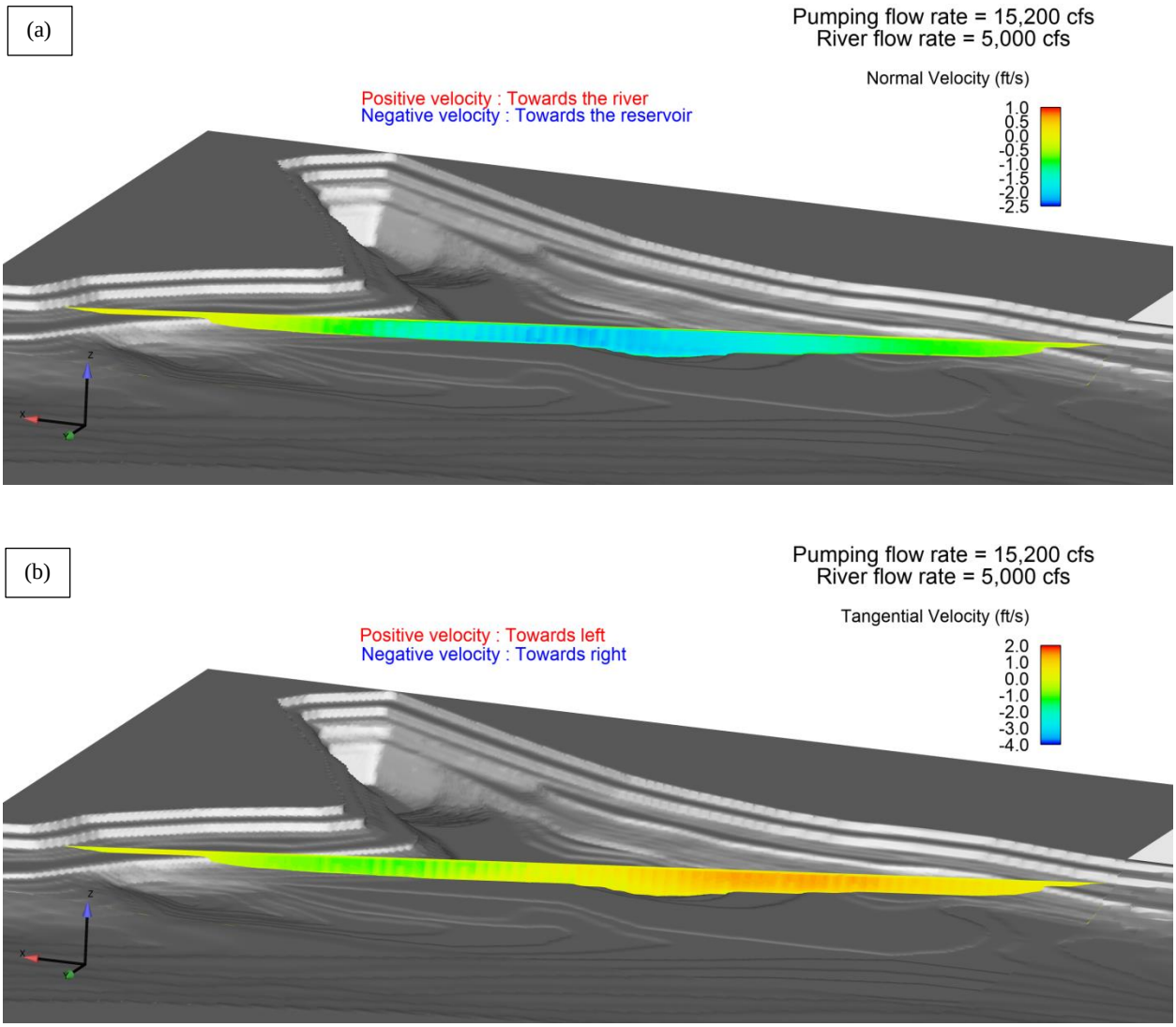

Figure 5-18. (a) The normal velocity, and (b) the tangential velocity; for the pumping case about 1 ft upstream of the net (side of the river) with flow rate = 15,200 cfs, river flow rate = 5,000 cfs, and water level 179 ft.

6.0 Additional Modeling Scenarios

After completing the modeling scenarios described in Section 5.0, additional sensitivity analyses were conducted to see if forces on the net could be reduced. Table 6-1 shows the additional modeling runs, which were conducted using a 0.75-inch mesh from top to bottom of the exclusion net.

Table 6-1: Additional CFD Modeling Scenarios

River Conditions	River Flow (cfs)	Water Level at Project Intake/Tailrace (ft)	Pumping Flow (cfs)	Mesh Size of net (inch)
Low River Flow, Low TFI Level	5,000	179	15,200	0.75
Low River Flow, Average TFI Level	5,000	181.4	15,200	0.75

The same CFD mesh as shown in Figure 4-1 was used. The velocity distribution in the horizontal plane for the above scenarios are shown in Figure 6-1 and 6-2. The normal and tangential velocity distribution in the vertical plane for the above scenarios are shown in Figure 6-3 and 6-4.

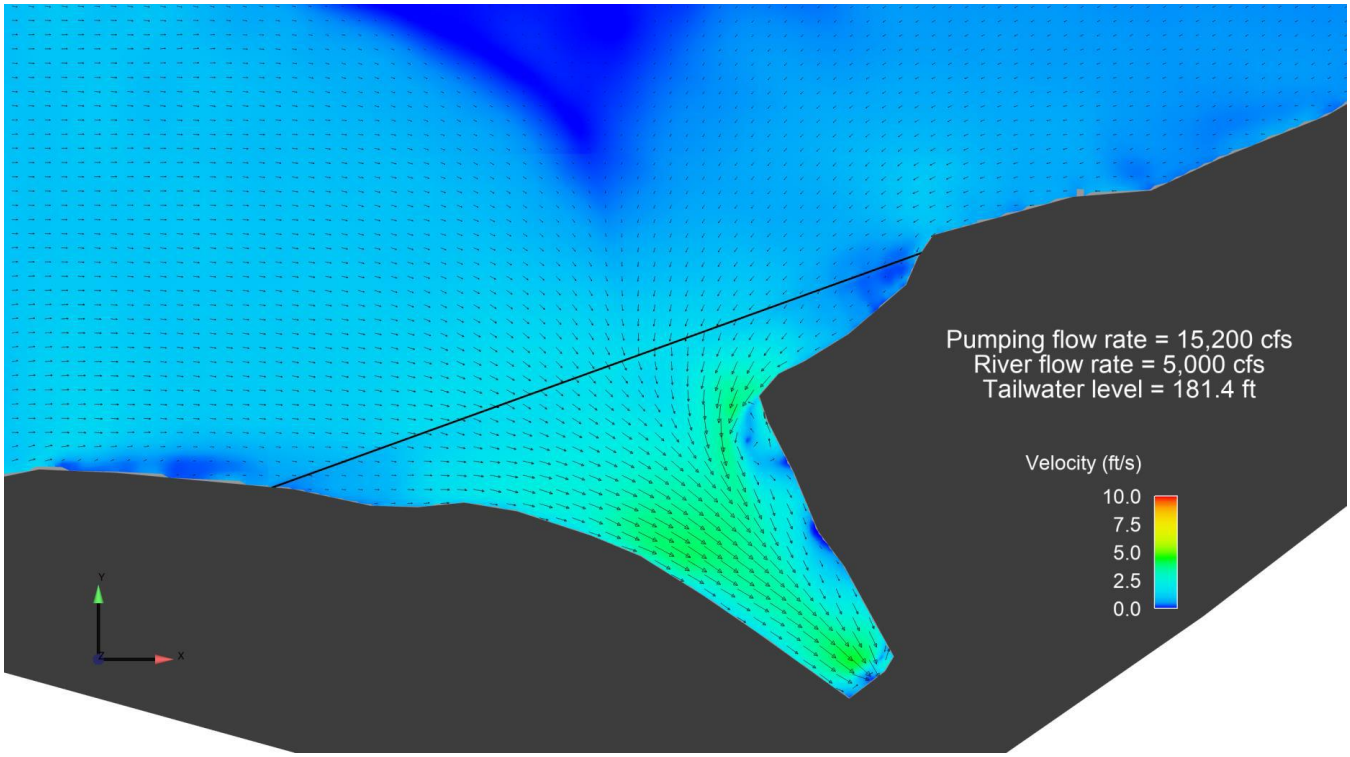

Figure 6-1. The horizontal velocity distribution for the pumping case at $z = 181$ ft with flow rate = 15,200 cfs, river flow rate = 5,000 cfs, water level= 181.4 ft and 0.75-inch mesh from top to bottom.

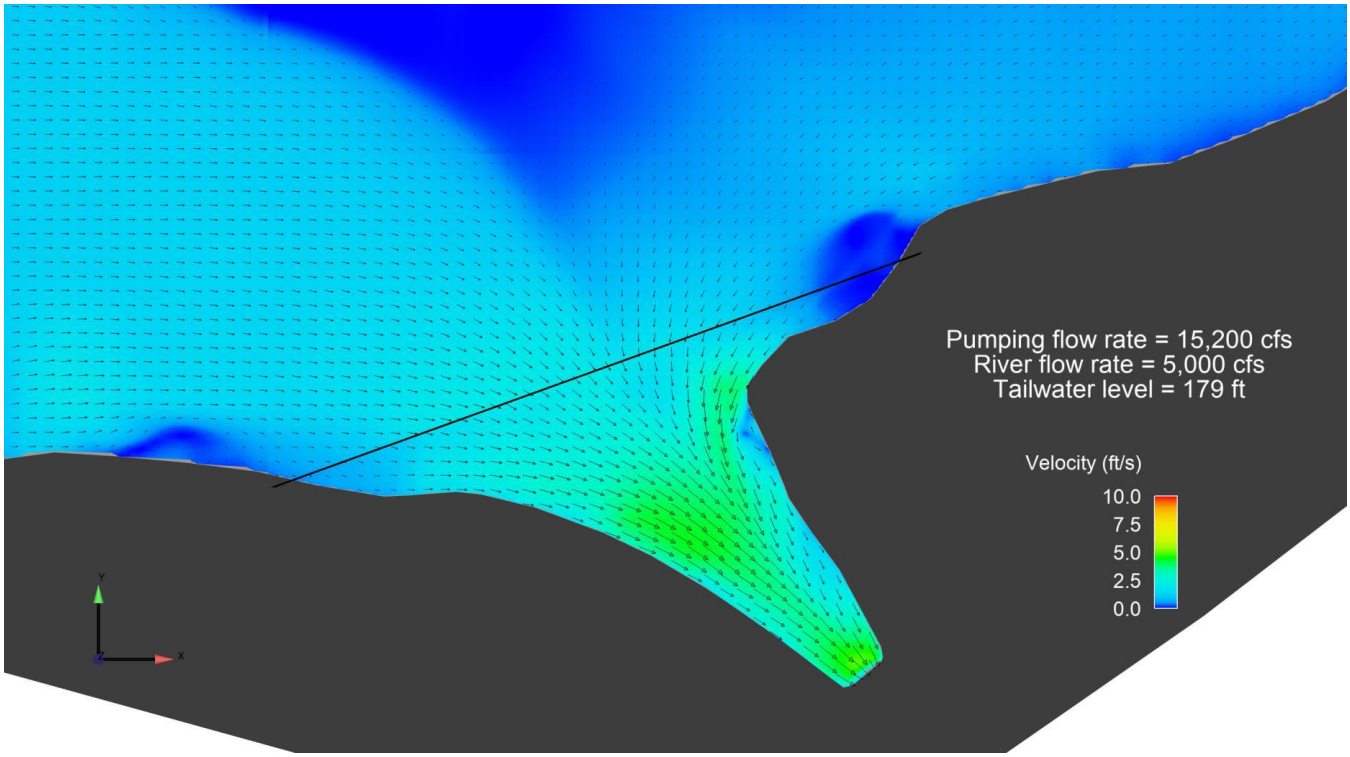

Figure 6-2. The horizontal velocity distribution for the pumping case at $z = 178$ ft with flow rate = 15,200 cfs, river flow rate = 5,000 cfs, water level= 179 ft and 0.75-inch mesh from top to bottom

Figure 6-3. (a) The normal velocity, and (b) the tangential velocity; for the pumping case about 1 ft upstream of the net (side of the river) with pumping flow rate = 15,200 cfs, river flow rate = 5,000 cfs, water level 179 ft, and ¾-inch mesh from top to bottom.

(a)

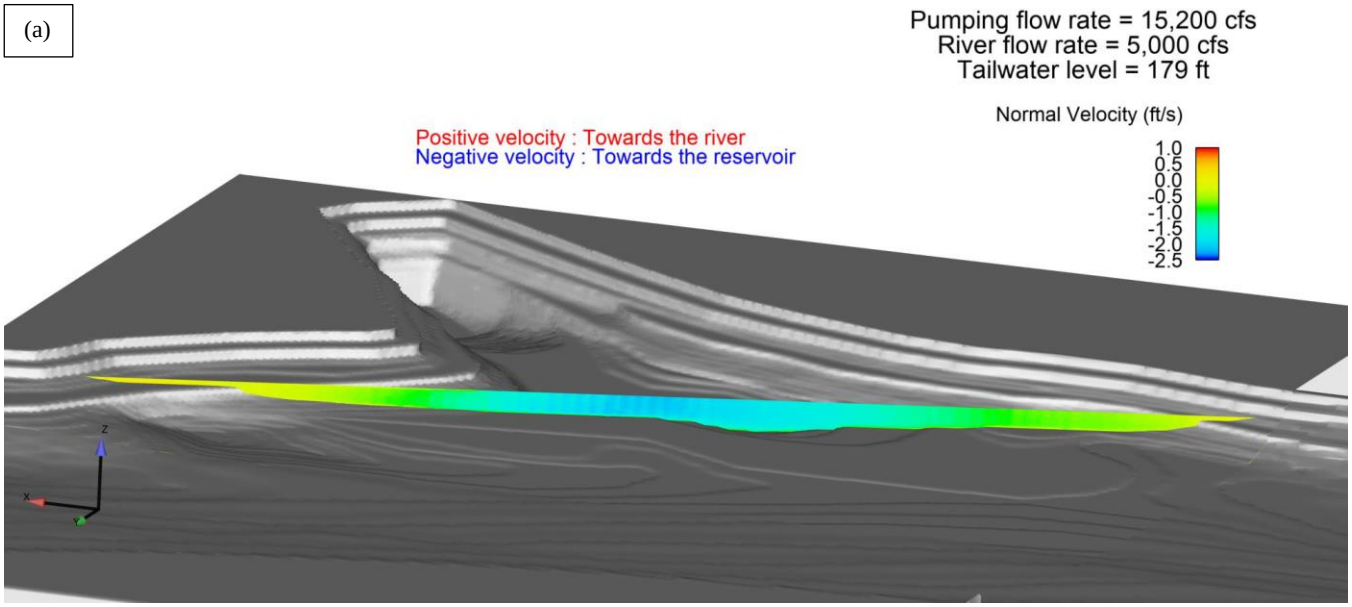

(b)

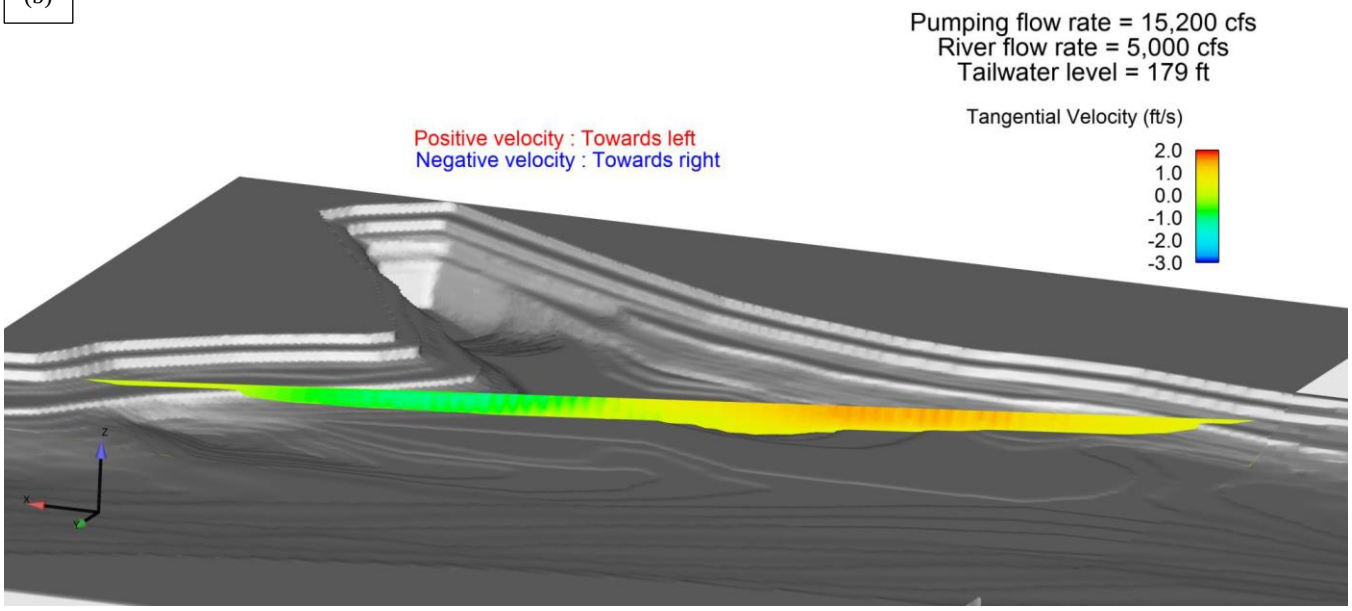

Figure 6-4. (a) The normal velocity, and (b) the tangential velocity; for the pumping case about 1 ft upstream of the net (side of the river) with pumping flow rate = 15,200 cfs, river flow rate = 5,000 cfs, water level 181.4 ft, and ¾-inch mesh from top to bottom.

(a)

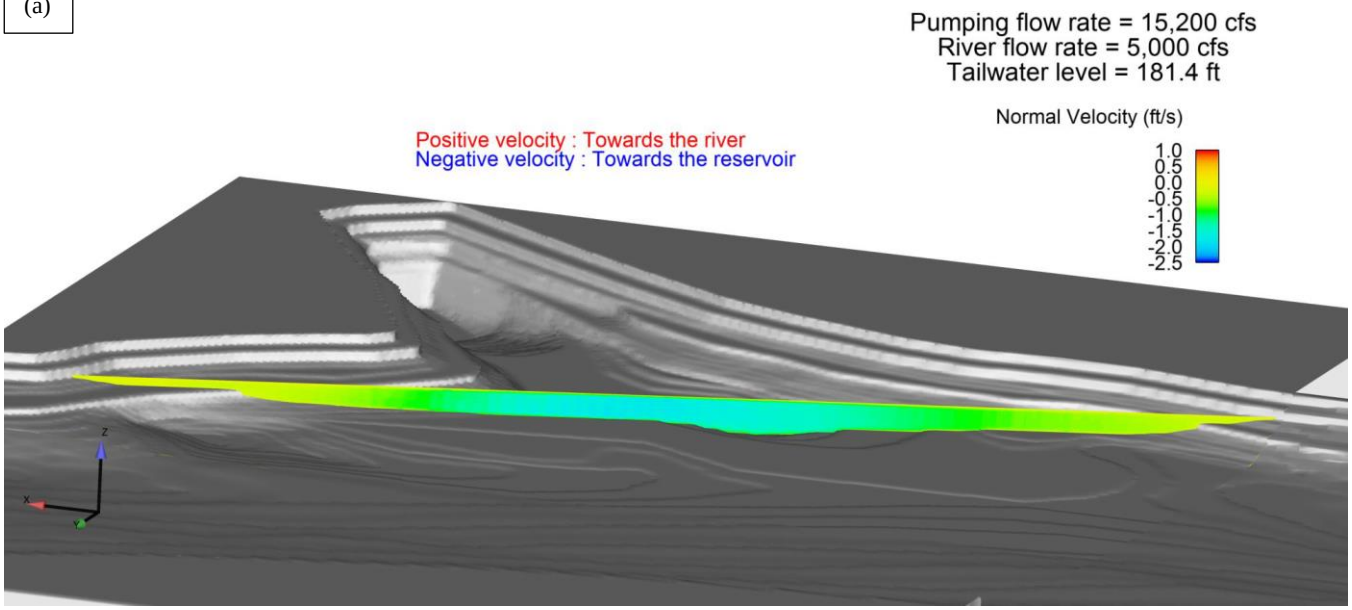

(b)

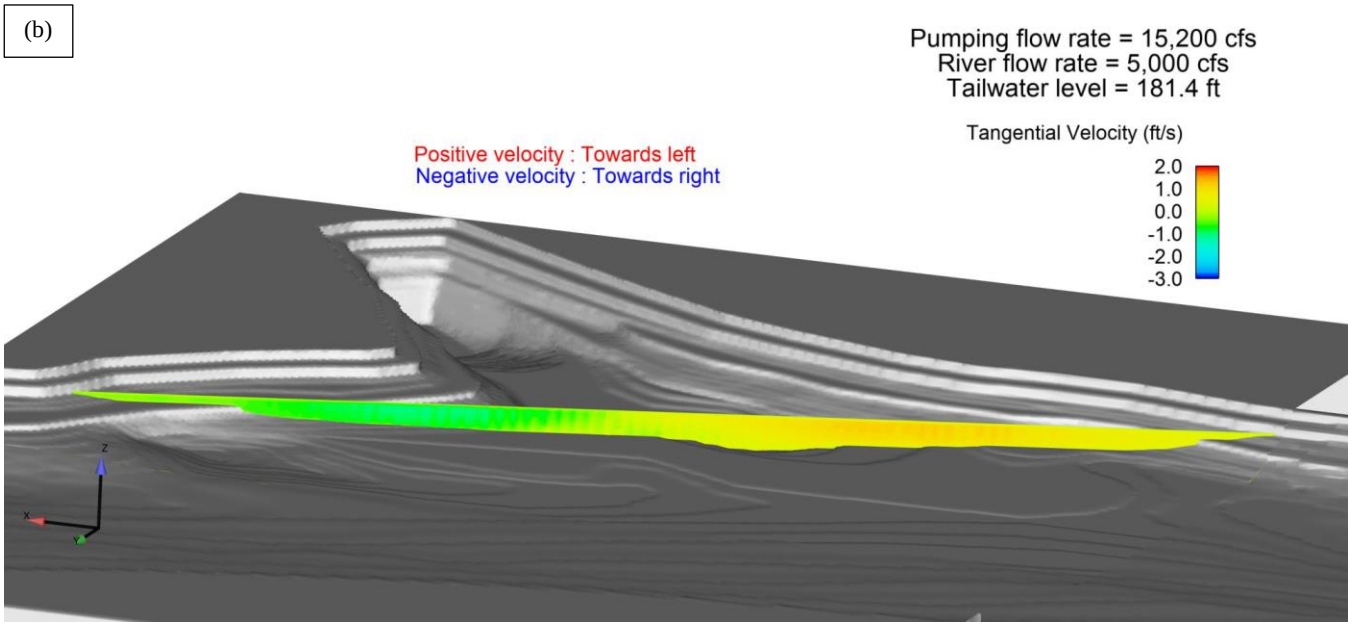

The results show that forces on the net are reduced with a larger 0.75-inch mesh from top to bottom. The forces on the net, as compared to the initial set of runs are summarized in Table 6-2.

Table 6-1. Summary of the pumping flow.

River Cond.	River Flow (cfs)	Water level Intake / Tailrace (ft)	Pump flow (cfs)	Mesh Size (inch)	Normal Force (lb)	Tang. Force (lb)	Avg. Normal Force per unit area (lb/ft^2)
Initial Modeling Runs							
High Flow	50,000	185	15,200	0.375 (top) 0.75 (bottom)	40,000	3,800	1.64
Medium Flow	30,000	182	15,200	0.375 (top) 0.75 (bottom)	45,000	3,100	2.13
Low Flow	5,000	179	15,200	0.375 (top) 0.75 (bottom)	32,500	600	1.91
Additional Modeling Runs							
Low Flow	5,000	179	15,200	0.75 top to bottom	10,000	106	0.56
Low Flow	5,000	181.4	15,200	0.75 top to bottom	8,800	40	0.45

7.0 Conclusions

For this study, drag and shear forces on exclusion net were calculated under different flow conditions. Six cases were taken into account, three generation cases for which the water is discharged into the river and three pumping cases for which water is pumped from the river into the impoundment. To study the forces on the exclusion net, numerical simulations were performed. In order to calculate forces acting on the net in the simulation model, drag coefficients and porosity of the exclusion nets were required. To determine the drag coefficients, first several sample nets with the same properties of the actual nets were deployed at the exclusion net locations at different depths of the water column. Sample net panels were removed from water at different times in order to account for the effect of algae growth and bio-fouling. Bio-fouling changes the permeability, drag coefficients and therefore the load on the exclusion net. These sample net panels were tested in the lab and their drag coefficients were determined for use in the numerical simulations. Results from CFD simulations performed in FLOW-3D showed that the highest calculated normal force on the exclusion net was ~60,000 lbs which occurred for the generation operation case at the time of low river flow. The maximum shear force is ~6,300 lbs for the generation case at the time of medium river flow.

It is important to note that in the numerical simulations it was assumed that the exclusion net is taut and occupies a flat vertical plane. In reality, the exclusion net would bow with the current. The assumption that the exclusion net is taut minimizes the cross-sectional area of flow in/out of the intake/tailrace. However, if the exclusion net bows significantly, its location will move, flow patterns through the exclusion net will be different and the open area of the net can change.

8.0 Next Steps

The next steps relative to the exclusion net include:

- Review results with National Marine Fisheries Service, United States Fish and Wildlife Agency and Massachusetts Division of Fisheries and Wildlife;
- Engage net manufacturer to understand design limitations;
- Explore potential modifications to the exclusion net layout to further reduce velocities and forces acting on the net;
- Start the design process for the exclusion net.

9.0 References

[1] Sedimentation Studies at the Connecticut River Intake/Tailwater. Alden Research Laboratory, Inc. January, 2015.

[2] Northfield Fish Protection Tailrace Barrier Net Drawings. "Northfield Tailrace Fish Protection Prelim Draft 7_13_17.pdf". Gomez and Sullivan Engineers. July 2017.

[3] Emails from Pacific Netting Products to Alden. Northfield Exclusion Net Drag Coefficient(s) and % blockage. Rich Pasma (Pacific Netting) to Mitch Peters (Alden). November 7 and 13, 2017.

[4] Schlichting, Hermann (1979), "Boundary Layer Theory", 7th Edition.

Appendix A Force Calculation Results

Table A-1. Exclusion net statistics for generation cases

	Upper Panel (3/8" Mesh)	Lower Panel (3/4" Mesh)	Both Panels
Generation, High River Flow, Low Turner Falls Impoundment level			
Normal Force (lbs)	34,200	6,300	40,500
Shear Force (lbs)	4,950	950	5,900
Normal pressure (lbs/ft^2)	2	0.83	1.63
Mean Normal Velocity (ft/s)	1.1	1.25	1.2
Mean Tangential Velocity (ft/s)	-1.2	-1.3	-1.25
Generation, Medium River Flow, Low Turner Falls Impoundment level			
Normal Force (lbs)	43,400	8,600	52,000
Shear Force (lbs)	5,400	900	6,300
Normal pressure (lbs/ft^2)	2.7	1.73	2.45
Mean Normal Velocity (ft/s)	1.65	1.35	1.5
Mean Tangential Velocity (ft/s)	-1.8	-1.2	-1.55
Generation, Medium River Flow, Low Turner Falls Impoundment level			
Normal Force (lbs)	55,500	4,500	60,000
Shear Force (lbs)	4,400	300	4,700
Normal pressure (lbs/ft^2)	3.75	1.95	3.49
Mean Normal Velocity (ft/s)	1.58	1.55	1.57
Mean Tangential Velocity (ft/s)	-1.16	-1.0	-1.12

Table A-2. Exclusion net statistics for pumping cases

	Upper Panel (3/8" Mesh)	Lower Panel (3/4" Mesh)	Both Panels
Pumping, High River Flow, Low Turner Falls Impoundment level			
Normal Force (lbs)	30,900	9,100	40,000
Shear Force (lbs)	3,050	750	3800
Normal pressure (lbs/ft^2)	1.82	1.2	1.64
Mean Normal Velocity (ft/s)	-0.8	-1.1	-0.95
Mean Tangential Velocity (ft/s)	-1.8	-1.55	-1.7
Pumping, Medium River Flow, Low Turner Falls Impoundment level			
Normal Force (lbs)	37,400	7,600	45,000
Shear Force (lbs)	2,600	500	3,100
Normal pressure (lbs/ft^2)	2.3	1.73	2.13
Mean Normal Velocity (ft/s)	-1	-1.15	-1.05
Mean Tangential Velocity (ft/s)	-1.3	-0.7	-1.1

Pumping, Medium River Flow, Low Turner Falls Impoundment level			
Normal Force (lbs)	29,500	3000	32,500
Shear Force (lbs)	590	10	600
Normal pressure (lbs/ft^2)	2	1.2	1.91
Mean Normal Velocity (ft/s)	-1.22	-1.35	-1.25
Mean Tangential Velocity (ft/s)	0.11	0.28	0.16